RECENT ADVANCES IN MODELING SWASH ZONE DYNAMICS: INFLUENCE OF SURF-SWASH INTERACTION ON NEARSHORE HYDRODYNAMICS AND MORPHODYNAMICS

M. Brocchini[1] and T. E. Baldock[2]

Received 12 October 2006; revised 5 June 2007; accepted 17 January 2008; published 29 July 2008.

[1] The role of the swash zone in influencing the whole nearshore dynamics is reviewed with a focus on the interaction between surf and swash zone processes. Local and global hydromorphodynamic phenomena are discussed in detail, and a description of the overall swash zone operation is given. The effects of swash zone boundary conditions are highlighted, together with the importance of surf zone boundary conditions. Major emphasis is placed on illustrating the interactions of various hydrodynamic modes which, in turn, control the swash and surf zone morphology. Finally, methods to account for swash zone processes in coastal models with different temporal and spatial resolutions are proposed.

Citation: Brocchini, M., and T. E. Baldock (2008), Recent advances in modeling swash zone dynamics: Influence of surf-swash interaction on nearshore hydrodynamics and morphodynamics, *Rev. Geophys.*, *46*, RG3003, doi:10.1029/2006RG000215.

1. INTRODUCTION

[2] The interest of coastal engineers and scientists in swash zone (SZ) dynamics has grown during the last 10–20 years, with a simultaneous increase in the range of the scales of the physical processes that have been investigated (i.e., from small-scale turbulence to the scales of the largest morphological features, such as ridge and runnel systems). SZ flows are of fundamental importance not only because of their local effects (e.g., beach face morphology, overwash and overtopping of barrier islands and coastal defense structures, and longshore sediment transport) but also because they can affect the surf zone dynamics as a whole [e.g., *Elfrink and Baldock*, 2002; *Brocchini*, 2006]. In particular, the SZ is a region where the final dissipation of short-wave (wind and swell) energy usually occurs, while low-frequency wave energy (typical wave periods between 30 and 300 s) is, generally, reflected back seaward. In addition, intense interaction between short waves and between short waves and long waves at the surf-swash boundary can lead to the generation and reflection of further low-frequency waves (LFWs) [*Watson et al.*, 1994; *Mase*, 1995]. These, in turn, are powerful agents of sediment transport as they remove from the area of interest large amounts of the sediment that is put into suspensions by the wind waves.

[3] Early work on SZ dynamics essentially focused on the maximal excursion of water on the beach, given the frequency and amplitude of the incident wave train [*Hunt*, 1959; *Holman*, 1986]. Estimates of the maximum runup is still one of the major goals for research in the field of coastal engineering, the interest being related to (1) the increasing availability of field data for predictive purposes [*Ruggiero et al.*, 2004; *Stockdon et al.*, 2006] or (2) the use of advanced techniques like photogrammetry, topographic data collection, and digital image-processing techniques, which largely improve shoreline detection capabilities [*Boak and Turner*, 2005] or (3) the mitigation of tsunamis-related hazards [*Li and Raichlen*, 2002; *Jensen et al.*, 2003].

[4] However, research based on the use of both laboratory [*Petti and Longo*, 2001] and field data [*Raubenheimer et al.*, 2004] is also focusing on the analysis of smaller-scale processes like the SZ internal kinematics and turbulence. The near-bed dynamics are attracting major interest in view of the predictions of bottom shear stress required for the evaluation of sediment transport [*Nielsen*, 2002]. The local sediment size, which strongly influences mechanisms such as the infiltration and exfiltration of water across the beach face [*Turner and Masselink*, 1998] and the response of the beach face itself [*Hughes and Cowell*, 1987], is also of major importance to the SZ morphological evolution. Consequently, the evolution of coarse- and finer-grained

[1]Istituto di Idraulica e Infrastrutture Viarie, Università Politecnica delle Marche, Ancona, Italy.
[2]Division of Civil Engineering, University of Queensland, Brisbane, Queensland, Australia.

8755-1209/08/2006RG000215$15.00
Paper number 2006RG000215

beaches is significantly different. For both beach types the prediction of the SZ dynamics and nearshore morphological evolution is becoming the main goal of SZ research [*Butt and Russell*, 2000], but other topics are receiving increasing attention, for example, the evaluation of the forces exerted by SZ flows on massive bodies [*Yeh*, 2006].

[5] A number of recent review papers on SZ flows have been devoted to specific issues, for example, SZ turbulence generation and decay [*Longo et al.*, 2002] and near-bed hydrodynamics and SZ sediment transport [*Elfrink and Baldock*, 2002]. Very recently, the 1st International Workshop on Swash Processes was held in Lisbon just prior to the 29th International Conference on Coastal Engineering. The results of the workshop were collected in a special issue of the international journal Continental Shelf Research, where further reviews of specific recent advances in SZ groundwater dynamics [*Horn*, 2006], in SZ morphodynamics [*Masselink and Puleo*, 2006], and in SZ modeling issues [*Brocchini*, 2006] can be found.

[6] The present review paper represents a further review of the scientific knowledge and modeling needed to properly account for the fundamental role of this narrow land-sea boundary. The specific aim of the present work is an extensive description of recent and ongoing research on SZ dynamics within the broader context of SZ processes since the latter has been absent from the recent reviews focused on specific topics.

2. MAIN FEATURES OF THE SZ DYNAMICS

[7] The oscillatory flows of the SZ are characterized by two main properties.

2.1. Intermittency

[8] The moving shoreline leads to alternate wet and dry regions, both in the vertical and tangential to the beach face. Hence, across the beach face, the flow depth and velocity are only defined for short intervals of time. In this perspective, the SZ is a very special boundary layer in which not only must small scales be properly resolved and their influence fed into the larger-scale dynamics, but the connection between small and large scales must be performed through special averaging methods. Such methods have been used to determine the interaction between short- and long-period progressive water waves by *Hasselmann* [1971] and to determine the SZ flows by *Brocchini and Peregrine* [1996] and *Brocchini and Bellotti* [2002]. The shoreline position, flow depths, and flow direction also vary in the longshore direction and are complex as a result of a mix of standing waves and edge waves [*Holland and Holman*, 1999]. Interactions between swash forced by oblique wave groups may induce additional large-scale variations in the shoreline position in the longshore direction [cf. *Baldock et al.*, 1997].

2.2. Shallow Depths

[9] The collapse of the flow on to a moving shoreline leads to flow depths at the runup tip [*Shen and Meyer*, 1963] and throughout the SZ that are very shallow in comparison to the horizontal length scale of the flow. The flow is approximately tangential to the beach surface, which allows application of the nonlinear shallow water equations (NSWE) with good confidence [*Peregrine*, 1972]. In these shallow intermittent flows, descriptions of the bed boundary layer and friction remain a challenge despite recent progress [*Cowen et al.*, 2003]. For example, in oscillatory wave boundary layers, the effects of friction in terms of energy dissipation and net sediment transport are usually described in terms of a friction factor that is constant over the wave cycle. However, this is not appropriate for SZ flows, where the initial conditions and flow depths for the uprush and backwash flows are very different.

[10] The complexity of the SZ dynamics suggests a first description be given by neglecting bottom friction and flow infiltration/exfiltration across the bed boundary. With this simplified approach, a runup event (single swash) resulting from an incident broken wave (surf zone bore) can be described by the following sequence:

[11] 1. At the breakpoint the wave, incident at an angle θ_b with the beach normal, starts dissipating its energy because of breaking-induced turbulence. As a consequence the wave height H decreases.

[12] 2. In the surf zone the wave height decreases, approximately in proportion to the water depth, and the change in depth induces a rotation of the wavefront by refraction. This is illustrated in Figure 1 where numerically computed waves propagate over a uniformly sloping beach and break with a relatively large angle θ_b between the bore path and the shore normal (top portion of the image). Refraction makes the wave angle decrease to a smaller value (θ_s) when the bore meets the shoreline (see bottom portion of the image).

[13] 3. As the bore height H_b approaches the local instantaneous shoreline (zero depth), the bore front and the water behind the bore front rapidly accelerate [*Whitham*, 1958], and the bore collapses [*Shen and Meyer*, 1963], with its potential energy being suddenly transformed into the kinetic energy of a thin wedge of water whose tip propagates up the beach face with initial velocity $u_0 = C\sqrt{gH_b}$, where g is gravitational acceleration and C is a coefficient describing the efficiency of the energy transformation during bore collapse in terms of a measure of the bore speed [*Baldock and Holmes*, 1999]. In reality, the bore collapse takes a small but finite time, during which the shoreline velocity increases to a maximum that corresponds to the initial uprush velocity. The motion of the swash front on a beach of slope γ is an approximate parabolic trajectory, where the shoreline position x_s is described by $x_s(t) = u_0 t - \frac{1}{2}\sin\gamma g t^2$, where t is the time since the collapse of the bore. An analytical solution of the NSWE exists for special initial conditions [*Shen and Meyer*, 1963] and describes a very shallow asymmetric swash flow. Numerical solutions for other initial conditions give larger flow depths and less asymmetry [*Hibberd and Peregrine*, 1979; *Guard and Baldock*, 2007];

[14] 4. For a sequence of waves approaching the beach, the degree of swash-swash interaction within the SZ

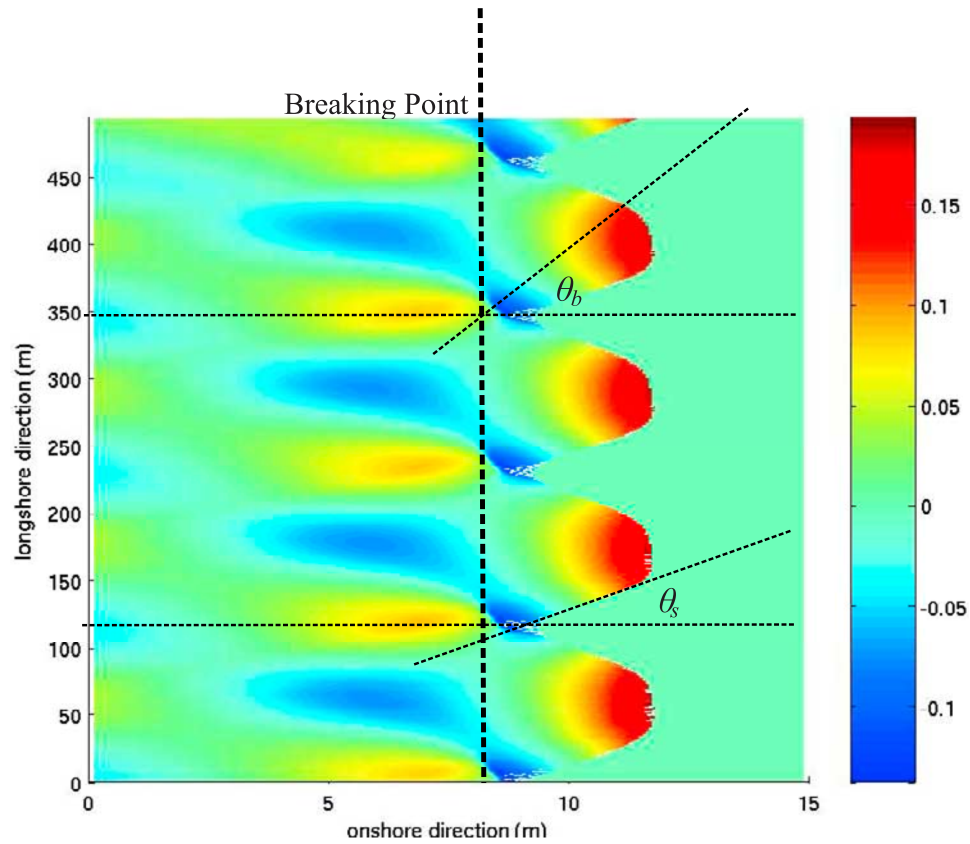

Figure 1. Periodic swashes: free surface patterns, breaking point, and angles of attack. The color bar gives the surface elevation values in meters.

depends on the ratio between the natural period of the individual swash events T_S and the incident wave period T; for $T > T_S$ little or no interaction occurs. Conditions for $T_S > T$ and for nonbreaking LFWs are discussed further in section 2.3.2.

[15] A more detailed and complete description of the SZ dynamics induced by breaking waves (the usual conditions on natural sand beaches) can, subsequently, be given to include all near-bed phenomena. Here this is qualitatively illustrated through Figures 2 and 3.

[16] Figure 2 shows conditions at the start of bore collapse and when the shoreline has advanced approximately half of the maximum runup distance up the beach. Following bore collapse, the water surface dips seaward, and the

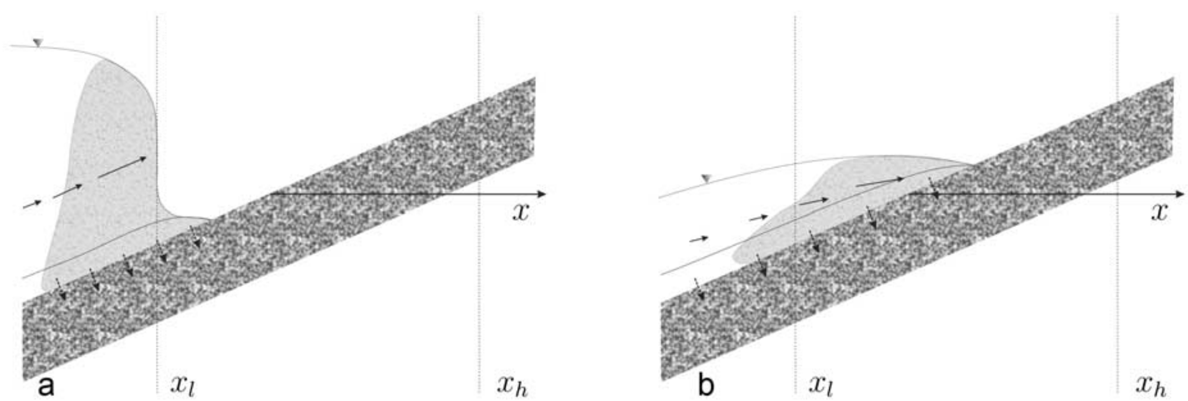

Figure 2. Runup phase of a swash event. (a) Bore collapse at $t = 0$. (b) Runup at $t \approx 2T_S/10$. The solid arrows at mid water depth indicate the intensity of the depth-averaged velocity, the dashed arrows at the bed indicate the direction of the water flow in the bed (downward indicates infiltration; upward indicates exfiltration), the solid line near the bed indicates the top of the bottom boundary layer, while the shaded area in the wave body indicates the region of highest sediment concentration and greatest shear stress. Here x_l and x_h are the lowest rundown and the highest runup, respectively, during a cycle.

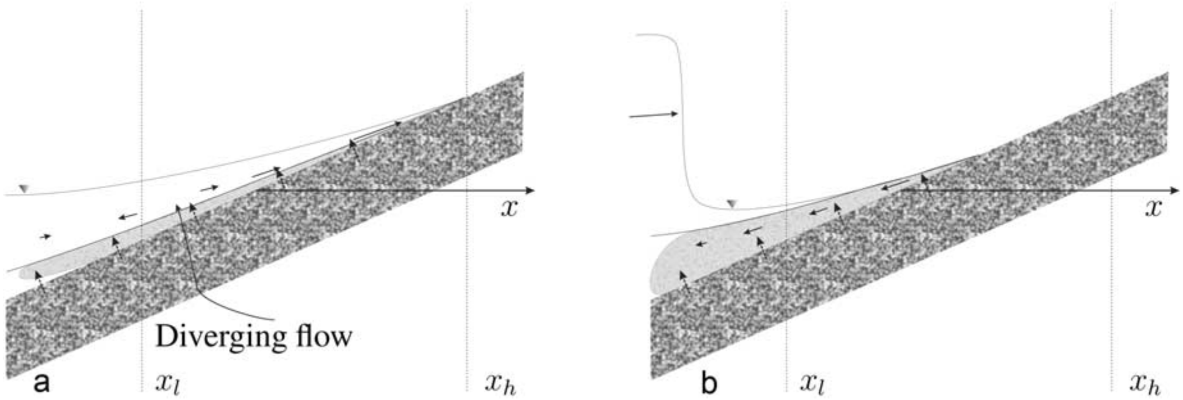

Figure 3. Run-down phase of a swash event. (a) End of the runup and beginning of rundown at $t \approx 4T_S/10$. (b) Rundown and subsequent incoming wave at $t \approx 8T_S/10$. For graphical elements, see Figure 2.

local and total flow acceleration are directed offshore for nearly the whole swash event (an exception occurs as the bore collapses) [*Baldock and Hughes*, 2006]. The boundary layer is therefore subject to a weak adverse pressure gradient during the runup. However, water infiltration into the bed contributes both to thinning the bottom boundary layer and to removing water available for the subsequent run-down phase [*Turner and Masselink*, 1998]. The above mechanisms and the intense flow velocity combined with a relatively thin boundary layer result in a relatively large shear stress on the seabed. Moreover, turbulence from the collapsing bore is advected into the SZ [*Yeh et al.*, 1989], such that presuspended sediment from the surf zone is added to the local sediment entrained within the SZ, so that a rather uniform distribution of sediment is found over the entire water column. During the runup, sediment transport occurs both as bed load and as suspended load of comparable strengths. The quantity of presuspended sediment appears very important in controlling the net sediment transport over the swash cycle [*Pritchard and Hogg*, 2005].

[17] Figure 3 illustrates the main features of the run-down phase; flow reversal commences first at the seaward end, and the boundary layer is subject to an increasingly stronger favorable pressure gradient. The divergence of the flow field that takes place around flow reversal reduces the swash further (see Figure 3a). Around flow reversal, the flow velocity is so weak that much of the suspended sediment settles, so that during rundown most of the sediment transport occurs as a sheet flow (see Figure 3b). The effect of exfiltration out of the seabed in thickening the boundary layer is counterbalanced by the thinning effect of the favorable pressure gradient [*Baldock and Hughes*, 2006]. The backwash flow quickly becomes supercritical; subsequently, the flow at a given location is not influenced by the next incident wave or bore until the next wave arrives at that position (see also Figure 13). A backwash bore may form toward the end of the backwash if no new incident wave arrives [e.g., *Peregrine*, 1974]. The influence of the backwash flow may extend offshore of the run-down position through the formation of a wall jet or backwash vortex [*Matsunaga and Honji*, 1980, 1983]. The supercritical nature of the flow is important in terms of swash-swash interactions and the generation of outgoing LFWs within the SZ.

[18] For fully developed bores approaching the shore, the shoreline motion closely approximates the general ballistic form of the analytical solution of *Shen and Meyer* [1963], particularly if friction effects are accounted for [*Hughes*, 1992, 1995; *Puleo and Holland*, 2001]. While originally proposed only for the close proximity of the moving shoreline, the Shen-Meyer solution (hereinafter SM63) is a valid solution of the NSWE over the full swash width and has recently been used to investigate overtopping swash flows [*Peregrine and Williams*, 2001] and sediment transport in the SZ [*Pritchard and Hogg*, 2005]. However, the SM63 solution is a particular solution of the NSWE for very special boundary conditions, which correspond to those for a dam-break wave on a sloping bed [*Pritchard and Hogg*, 2005]. In terms of the characteristic form of the NSWE, the solution is governed by a specific and constant value ($\alpha = 2$) of the Riemann invariant on the incoming characteristics [*Peregrine and Williams*, 2001]:

$$\left(\frac{\partial}{\partial t} + (u + c)\frac{\partial}{\partial x}\right)(u + 2c + t) = 0 \tag{1}$$

$$\left(\frac{\partial}{\partial t} + (u - c)\frac{\partial}{\partial x}\right)(u - 2c + t) = 0. \tag{2}$$

where u is the free-stream velocity, c is the shallow water wave celerity, and x is the spatial coordinate parallel to the beach face and inshore pointing.

[19] Introducing the characteristic variables $\alpha(x, t)$ and $\beta(x, t)$ gives

$$\frac{d\alpha}{dt} = 0 \qquad \text{on} \qquad \frac{dx}{dt} = u + c \tag{3}$$

$$\frac{d\beta}{dt} = 0 \qquad \text{on} \qquad \frac{dx}{dt} = u - c, \tag{4}$$

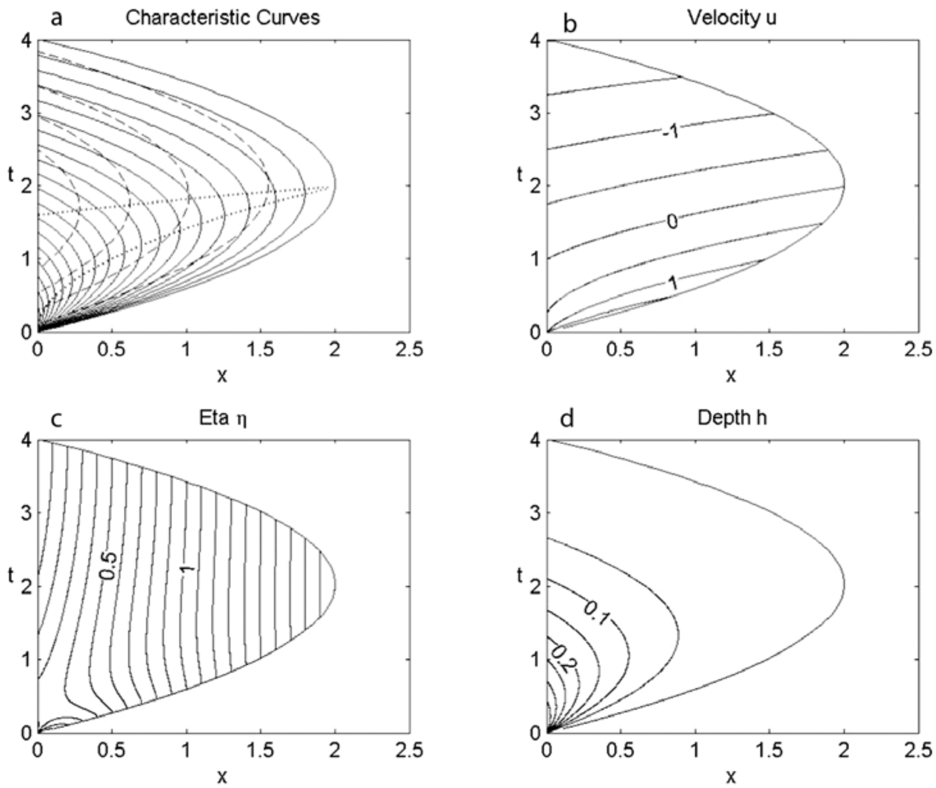

Figure 4. (a) Characteristic curves, (b) contours of flow velocity, (c) surface elevation, and (d) depth for the SM63 solution. Dotted lines in Figure 4a show locus of $u = c$ (critical flow) for uprush and backwash. Adapted from *Guard and Baldock* [2007], reprinted with permission from Elsevier.

where

$$\alpha(x,t) \equiv u + 2c + t, \qquad \beta(x,t) \equiv u - 2c + t. \tag{5}$$

Equation (3) describes the forward C_+ (or advancing) characteristics, and equation (4) describes the backward C_- (or receding) characteristics. The SM63 swash solution neglects the initial momentum of the water behind the bore front and limits the surf zone region from which flow enters the swash to 1/16 of the swash runup length [see *Pritchard and Hogg*, 2005, Figure 1]. The flow volume entering the swash is small, resulting in a very thin swash, which is not representative of field or laboratory observations [*Baldock et al.*, 2005].

[20] *Guard and Baldock* [2007] present numerical solutions of the characteristic equations for varying $\alpha(t)$ on the incoming C_+ characteristics, which are equally valid solutions for the characteristic form of the NSWE (3) and (4). The physical interpretation is that the different solutions for varying $\alpha(t)$ correspond to different mass and momentum fluxes at the seaward boundary and different flows within the SZ. In contrast, the SM63 solution gives similar flow conditions for all swash events for a particular beach slope and runup amplitude [*Peregrine and Williams*, 2001]. Consequently, the SM63 swash solution results in a single net sediment transport pattern for the same sediment and presuspended sediment concentration, irrespective of the surf zone wave conditions [*Pritchard and Hogg*, 2005]. In reality, the inner surf zone hydrodynamics are very important boundary conditions for the swash [*Elfrink and Baldock*, 2002]. Figures 4 and 5 contrast the flow patterns for the SM63 solution ($\alpha = 2$, which is equivalent to the dam-break solution on a slope) and the solution for $\alpha = 2 + t$ on the swash boundary, which is appropriate for fully developed, near-uniform bores, respectively. Whitham's rule [*Whitham*, 1958] may also be used to describe the incident bore and seaward boundary condition and gives a similar solution to that shown in Figure 5. Figures 4b and 5b show that flow reversal occurs much later with the new solution, indicated by the locus of $u = 0$, and water enters the SZ from much farther seaward than proposed by *Pritchard and Hogg* [2005]. Consequently, the water depth in the SZ is also much greater in the new solution (compare contour values and positions in Figures 4d and 5d).

[21] The solution obtained with the more realistic boundary values represents much deeper swash flows and a less asymmetric flow velocity between uprush and backwash, conditions which favor more shoreward transport in comparison to the SM63 solution. The longer period of inflow also enables greater quantities of sediment from farther offshore to be advected into the SZ. *Pritchard and Hogg* [2005] show that this is a very important factor in the net sediment flux into and out of the SZ. In addition, converging flow can occur toward the end of the backwash for increasing $\alpha(t)$, such that the advective acceleration can be positive, even though the total acceleration remains negative (offshore). The flow convergence may have implications for the transport and deposition of suspended sediment in the

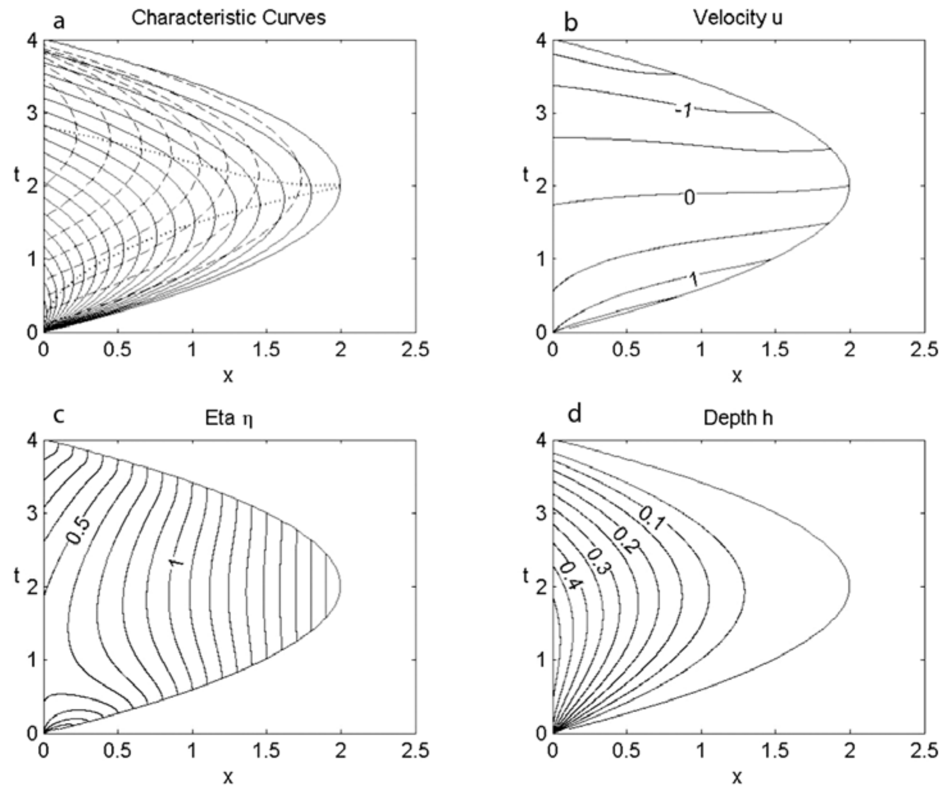

Figure 5. (a) Characteristic curves, (b) contours of flow velocity, (c) surface elevation, and (d) depth for $\alpha(x_b, t_b) = 2 + t_b$. Dotted lines in Figure 5a show locus of $u = c$ (critical flow) for uprush and backwash. Adapted from *Guard and Baldock* [2007], reprinted with permission from Elsevier.

lower SZ. In a related application, *Yeh* [1991] used the SM63 solution to describe the shoreline runup of tsunami bores. *Guard et al.* [2005] contrast the SM63 solution and alternative solutions for tsunami-scale runup based on the solution procedure above. Again, much deeper tsunami flow depths are predicted.

2.3. Low-Frequency Wave and Swash-Swash Interactions

[22] Both nonlinearity and groupiness of short waves are the major mechanisms responsible for the generation of LFWs. These waves can be either "bound" to a group of short waves (i.e., propagating at the group velocity [see *Longuet-Higgins and Stewart*, 1964]) or "free." The free long waves may be bound waves released from the group structure by short-wave breaking (see Figure 6) or may be formed by short waves interacting in the SZ [*Watson et al.*, 1994] (see also Figure 7, right) or may be breakpoint-forced long waves [see, e.g., *Baldock*, 2006, and references therein]. The latter are forced by time-varying radiation stress gradients that are generated as the wave breaking point oscillates onshore and offshore during the passage of groups of low and high waves.

2.3.1. Swash-Swash Interactions

[23] The shoreline boundary imposed by the beach face is different from that imposed by a vertical wall (see Figure 7) and leads to the partial reflection of the remaining incident wave energy, particularly the LFWs generated by offshore wave groups and during the breaking process [*Guza and Thornton*, 1985].

[24] LFWs frequently dominate swash flows on both mildly sloping and steep beaches, but the precise mechanisms differ subtly and depend primarily on the relative beach slope in the surf and swash zones, characterized by the Iribarren number, $\xi = \gamma/\sqrt{(H_0/L_0)}$, where H_0 and L_0 are the deepwater wave height and wavelength, respectively, and Miche parameter, $\varepsilon = a_S\omega^2/(g\gamma^2)$, respectively, where a_S is the vertical amplitude of the shoreline motion, $\omega = 2\pi/\mathrm{T}$, and γ is slope, and it is assumed that $\tan(\gamma) \approx \gamma$. The Miche parameter is a measure of the ratio of the shoreline acceleration to the downslope gravitational acceleration and can also be regarded as a swash similarity parameter. Note that while the Iribarren number is used to characterize surf zone conditions on the basis of offshore wave properties, the Miche parameter characterizes the SZ conditions on the basis of near-shoreline wave properties, a_S/γ being a measure of the horizontal wave runup at the shoreline. On dissipative beaches (low ξ), standing LFWs dominate the shoreline motions because the short-wave energy is dissipated in a saturated surf zone where the short waves are depth limited. Nonbreaking standing LFWs are limited to $\varepsilon < 1$ [e.g., *Brocchini and Peregrine*, 1996], but large-amplitude swash motions can occur at these frequencies, with corresponding high-velocity flows [*Guza and Thornton*, 1985].

[25] On reflective beaches (higher ξ), LFWs may still dominate the shoreline motion, but in addition to the standing LFWs, there is a significant contribution from frequency downshifting in the surf zone [*Mase*, 1995],

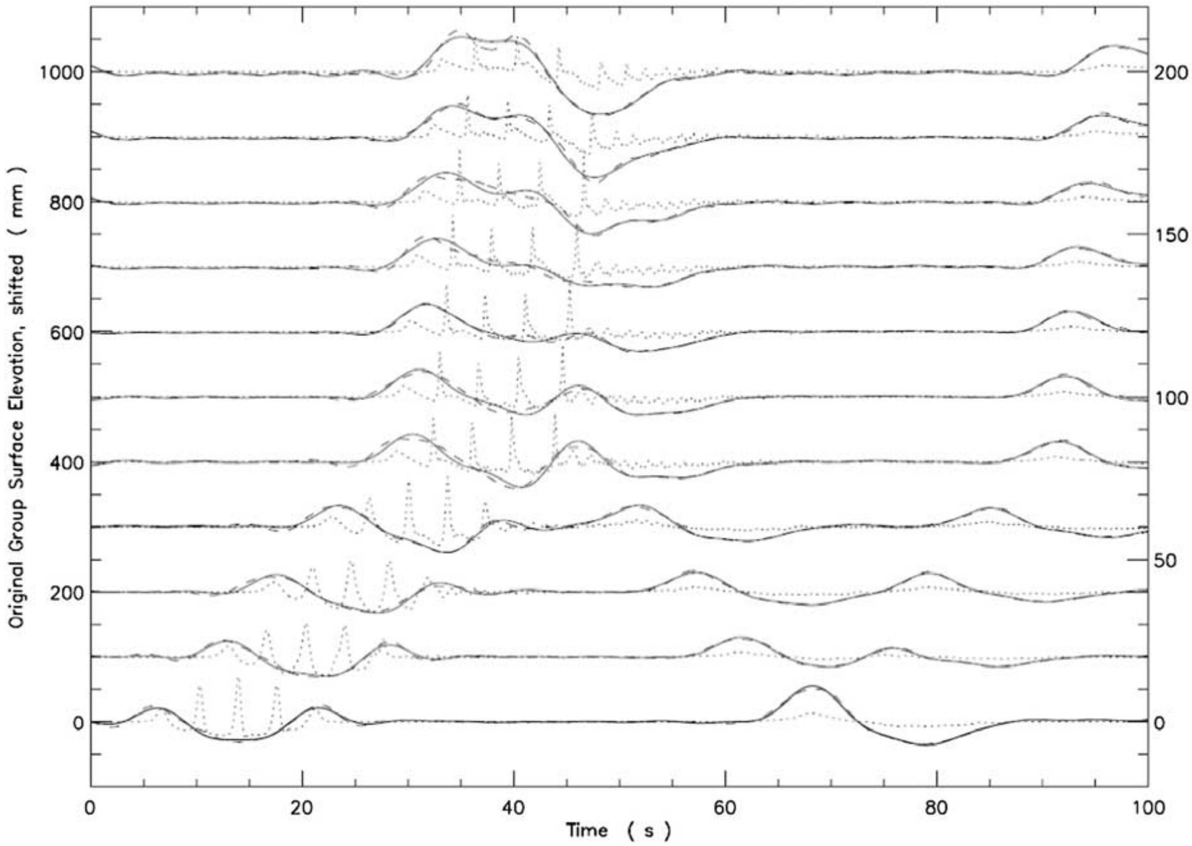

Figure 6. A wave group (thin dashed lines) on a 1:100 beach, with the Fourier (heavy dashed lines) and wavelet (solid lines) filtered signals magnified and superimposed. Adapted from *Barnes* [1996].

wave grouping remaining in the unsaturated inner surf zone and swash-swash interactions [*Baldock et al.*, 1997]. Frequency downshifting occurs because the waves are not so strongly depth limited, with larger waves propagating faster than smaller waves as the bore speed increases above the linear shallow water wave speed. Swash-swash interaction occurs between incident waves (with period T) and the runup or backwash of preceding waves. The interaction generates a range of scales of new motion, from mean flows (swash setup) to LFWs, backwash bores and hydraulic jumps, and turbulence. For swash forced by noninteracting collapsing bores, and neglecting friction, the natural swash period T_S is a function of the bore height and speed at the mean water level shoreline, the beach slope, and gravitational acceleration [*Baldock and Holmes*, 1999]. Using this relationship, it is possible to quantify the degree of swash-

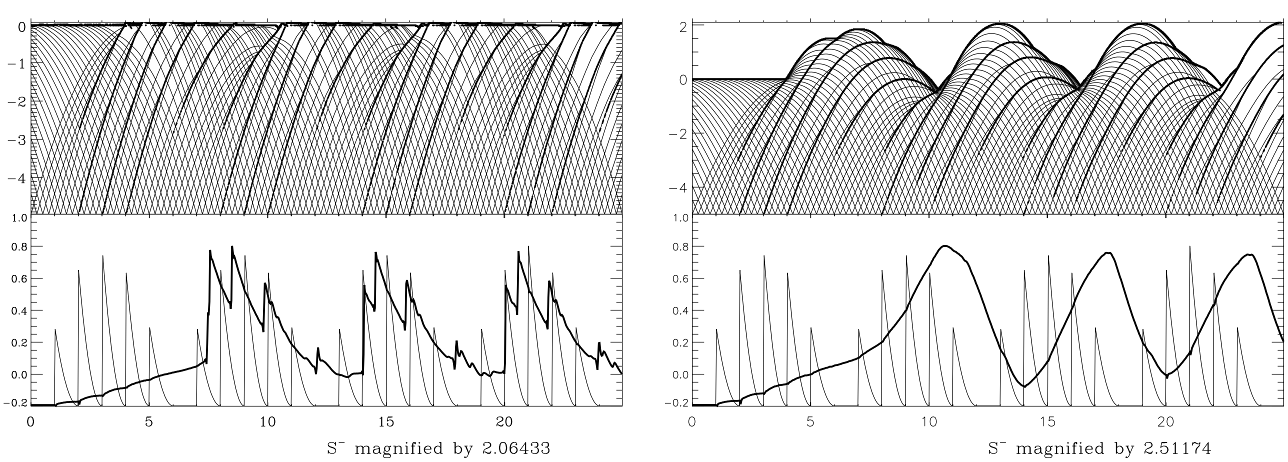

Figure 7. Illustration of the role of the SZ in generating/reflecting LFWs. (left) Wave groups reflected at a wall. (right) Wave groups generating a SZ. Adapted from *Bellotti and Brocchini* [2005], reprinted with permission from Elsevier.

swash interaction through a parameter of the form $\hat{T} = T_S/T$, where small values of $\hat{T}$ correspond to no interaction and values of $\hat{T}$ greater than or equal to 1 correspond to strong interaction. For monochromatic waves, the maximum swash amplitude is limited by interaction with preceding and following uprush and backwash, with the result that an increase in the incident bore height does not lead to an increase in the swash amplitude; that is, the swash is saturated. This is analogous to the concept of a saturated surf zone, where wave breaking limits the wave height in the nearshore region, irrespective of increases in the offshore wave height. Swash saturation, i.e., overlap of following swashes, occurs once $\hat{T} = 1$, which theoretically occurs when $\varepsilon \approx 2.5$ [*Baldock and Holmes*, 1999], in good agreement with a range of laboratory and field data. Swash saturation appears to occur within the wind and swell frequency bands on most natural beaches [*Huntley et al.*, 1977].

[26] Since the bore height and resulting runup at the shoreline is a function of the dissipation in the surf zone and, hence, a function of ξ, it is more useful to quantify the degree of swash interaction in terms of offshore wave conditions, which are the parameters most widely available. This can be done by equating the swash runup based on the initial velocity of the shoreline [*Baldock and Holmes*, 1999] with the swash runup obtained from derivatives of Hunt's formula: $R = KH_0\,\xi$. K is an empirical factor that varies with beach type, but a value of $K \approx 0.6-0.8$ is representative of a wide range of beach types and wave conditions [*Stockdon et al.*, 2006]. This gives

$$\hat{T} = 2\left(\frac{2}{\pi}\right)^{1/4}\left(\frac{K^2H_0}{gT^2\gamma^2}\right)^{1/4}, \qquad (6)$$

and the degree of swash interaction changes quite rapidly with changes in the beach face slope [*Puleo and Holland*, 2001] and wave period and to a lesser extent with changes in wave height. $\hat{T}$ is usually greater than 1 except for long-period swell on fairly steep beaches.

[27] The interaction between the short-wave runup and standing long waves in the SZ is complex but very important in terms of both the hydrodynamics and beach face morphology. The long waves move the short-wave runup zone across the beach face in a similar manner to the tide, significantly increasing the active SZ width. Short-wave runup (or backwash) may coincide with the runup (or drawdown) of the standing wave, increasing swash amplitudes and flow velocities through constructive interference. Destructive interference occurs if runup and backwashes oppose each other. Variations in the height of the incident bores also increase the active swash width, with the strength of the backwash from the preceding swash also influencing the next wave.

2.3.2. LFW Generation in the Swash

[28] The presence of standing long waves in the SZ and inner surf zone from incident and reflected LFWs makes it difficult to determine if further LFWs are generated within the SZ itself. Most suitable data show that the radiated LFWs are closely correlated reflections of the incident wave in the inner surf zone [*Baldock and Huntley*, 2002; *Battjes et al.*, 2004], suggesting LFW generation in the swash is not intense.

[29] Numerical modeling [*Watson et al.*, 1994] suggests that for individual wave groups the radiated wave in the inner surf zone is a maximum when the natural swash period and the period of the incoming wave groups (T_G) coincide and decreases rapidly for other ratios. T_S/T_G may be written as $\hat{T}_G = \hat{T}/N$, where N is the number of short waves in the wave group. However, $\hat{T}$ is of the order of 1–3 for a wide range of wave conditions and beach slopes; thus N must be also small (1–3) for $\hat{T}_G$ to be close to unity. Hence, in the SZ, significant LFW generation through short-wave interactions seems likely only for very short wave groups. This appears consistent with the supercritical flow conditions that occur for much of the backwash. The supercritical flow cannot decelerate to the subcritical conditions required for the smooth radiation of LFWs (which is a subcritical flow) without a hydraulic jump and significant energy dissipation occurring in the lower SZ. Therefore, while variations in incident bore height lead to large-amplitude low-frequency motions of the shoreline [*Mase*, 1988; *Baldock et al.*, 1997], these do not necessarily radiate LFWs of corresponding magnitude. However, the swash-swash interactions modify the shoreline boundary conditions for the incident long waves by moving the mean shoreline position farther shoreward, with an associated shoreward shift of the long-wave reflection position and the cross-shore position of the resulting standing wave.

2.4. Near-Bed Dynamics and Morphological Evolution

[30] The development and application of boundary layer models for the SZ has been attempted [*Packwood and Peregrine*, 1981], but large discrepancies in shear stress terms result in comparison to more conventional steady flow shear stress models. The bed shear stress is inversely related to the flow depth, more strongly so for a laminar boundary layer than for a turbulent boundary layer. Consequently, for a given flow velocity, shear stresses are proportionately larger at the leading edge than elsewhere in the flow. The shear stress can be expected to drop rapidly behind the front, particularly for a laminar boundary layer, and then increase again toward the end of the backwash.

[31] Measurements of the bed shear stress in swash flows are very limited. Various authors [*Cox et al.*, 2000; *Cowen et al.*, 2003; *Masselink et al.*, 2005] inferred bed shear stresses by fitting a log law to measured data from field and laboratory studies. Back-calculated estimates of friction factors were found to be larger in the uprush than for the backwash, consistent with a thinner boundary layer during the uprush. However, *Raubenheimer et al.* [2004], using a similar methodology applied to field measurements, found little difference between uprush and backwash friction factors. *Conley and Griffin* [2004] reported direct measurements of bed shear stress in the field using a hot film anemometer calibrated under steady flow over a smooth

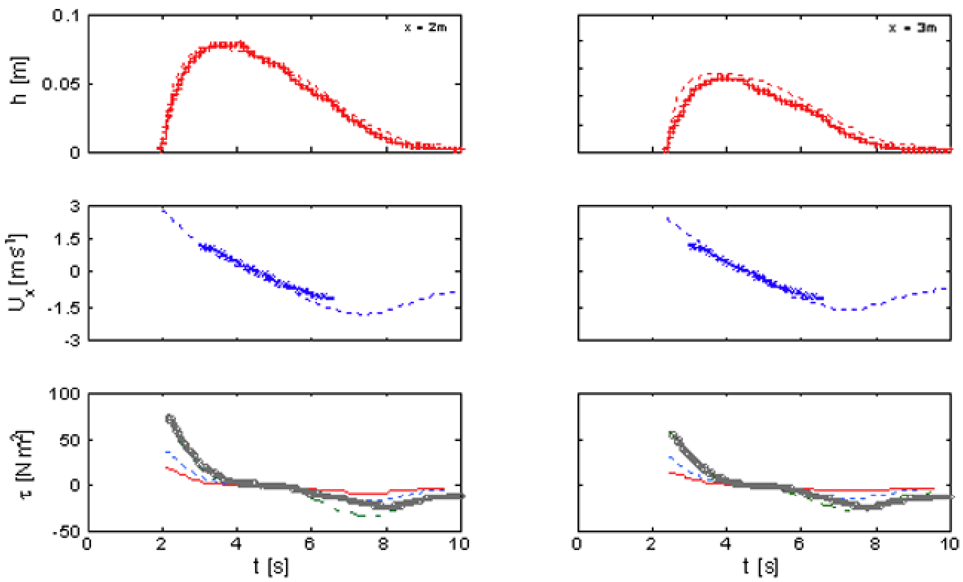

Figure 8. Swash flow and direct bed shear stress measurements on a plane smooth 1:10 slope laboratory beach. Data at (left) $x = 2$ m and (right) $x = 3$ m shoreward of the still water line. (top) Depth (h). (middle) Tangential velocity (U_x). (bottom) Bed shear stress (τ). Measured data are indicated by symbols; model results are indicated by lines. Predicted bed shear stresses are shown using a constant friction factor with $C_f = 0.005$ (solid line), 0.01 (dashed line), and 0.02 (dash-dotted line). Adapted from *Barnes and Baldock* [2007], reprinted with permission from Coastal Education and Research Foundation, Allen Press Publishing Services.

bed; moreover, they found significant differences between the uprush and backwash friction factors, but their friction factor estimates are an order of magnitude smaller than for other studies. This discrepancy has yet to be resolved. A possible reason may be the difficulty in determining the appropriate relationship between heat transfer and the bed shear stress in unsteady flows over mobile beds.

[32] Direct measurement of bed shear stress using a shear plate displaced in the direction of the applied stress has been widely used under steady flows and wave motion [*Riedel and Kamphuis*, 1973; *Grass et al.*, 1995; *Myrhaug et al.*, 2001]. In the swash, application of this technique is complicated by the intermittent nature of the flow, which can lead to hydrostatic loading on the plate and pressure gradients on the plate boundaries that vary very rapidly with time. *Barnes and Baldock* [2007] have attempted to address these issues and present laboratory-scale shear plate measurements from intermittent dry-wet bed dam-break flows and swash uprush and backwash flows. The dam-break data represent conditions analogous to the leading tip of the swash uprush.

[33] Figure 8 shows an example of the measured bed shear stress during uprush and backwash of a long bore. The data are corrected for the pressure gradient force on the plate boundaries using pressure measurements inside the shear cell, which is important in the inner surf zone and at the surf-swash zone boundary. These direct shear stress measurements show a pattern consistent with previous estimates as summarized in the discussion above. The shear stress is very asymmetric, with the maximum uprush bed shear stress more than twice that in the backwash. In addition, at this scale, the influence of friction is evident in the latter stages of the swash backwash when the flow depth becomes very small and the shear stress reduces slowly back to zero. Using a constant friction factor C_f over the whole swash cycle to calculate the shear stress ($\tau = 0.5\rho C_f U^2$, where ρ is the fluid density and U is a representataive stream velocity) provides a poor fit to the measured stress data. In fact, the measured shear stress is consistent with a rapidly varying friction factor, so the usual assumption in sediment transport models of a constant friction factor over the cycle or over the individual uprush and backwash cycles is not appropriate [see also *Cowen et al.*, 2003]. This is also true for the direct shear stress measurements at the leading edge of the dam-break flows. At a point, the local Reynolds number varies rapidly with time, and simultaneously, the friction factor varies as the flow progresses (Figure 9).

[34] This behavior might be expected on the basis of classical experimental data, where the friction factor for smooth beds is proportional to $Re^{-1/4}$. Both the swash data and dam-break data result in higher shear stresses at the runup tip than is suggested by classical steady flow open channel flow theory for equivalent Reynolds numbers and relative roughness. Equivalently, the friction factor at the leading edge of these dry-wet flows is 1.5–2 times that expected for steady flows (Figure 9). At present, no good models exist to describe this increase in the shear stress over that expected for steady flows, but it is likely to be related to the timescales over which the boundary layer develops, and this may be different for uprush and backwash [e.g., *Masselink et al.*, 2005]. The boundary layer behavior and shear stress will be dependent on the history of the flow

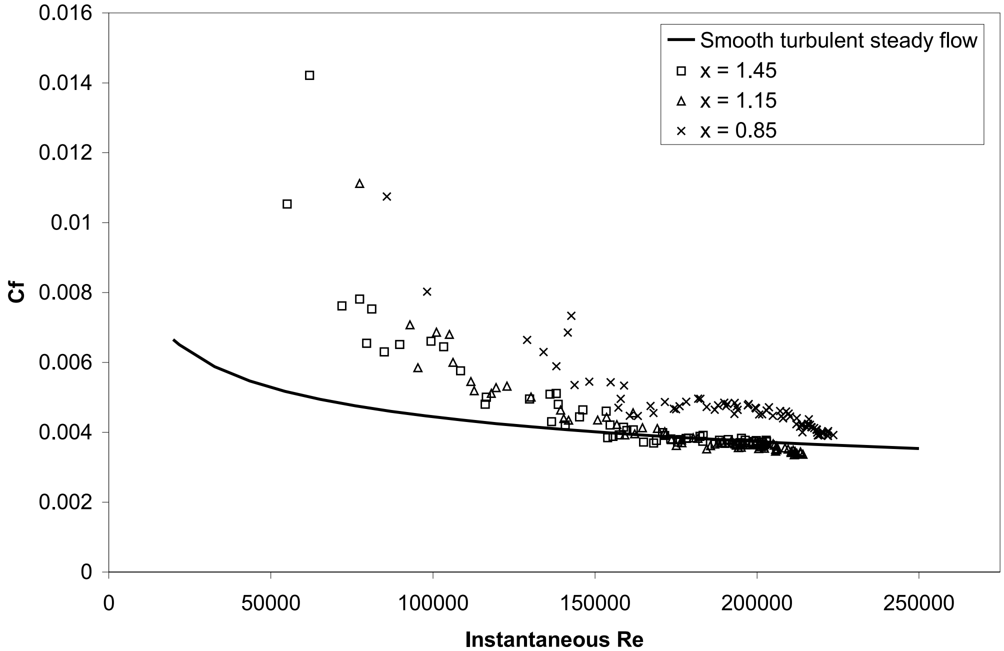

Figure 9. Friction factors (C_f) derived from direct shear stress measurements from dam-break flow over a smooth plane horizontal bed. Data correspond to measurements from different distances down from the dam position. Reynolds number is determined from the instantaneous local flow depth and flow velocity. Solid line indicates friction factors for steady flows at the same Reynolds numbers. Adapted from *Barnes and Baldock* [2007].

through the inner surf zone and following bore collapse, which is not likely to be well described by models applied in a stationary (Eulerian) reference frame. This point is considered further in section 4 with respect to future research. For mobile beds, the prediction of the bed shear stresses is further complicated by interaction between the granular moving layer (sheet flow) and the fluid, which requires a two-phase flow analysis. In this instance, discrete particle modeling is a promising approach at microscales [*Calantoni and Puleo*, 2006] but is beyond present computing power for practical applications.

[35] Present sediment dynamics models, based on the flow velocity (usually cubed) and an empirical friction factor, provide a good overall description of the sediment flux [*Masselink and Hughes*, 1998] but cannot adequately predict the fine balance between uprush and backwash sediment flux as a result of the flow skewness and asymmetry [*Masselink and Hughes*, 1998; *Butt and Russell*, 1999]. Direct measurement of the total net swash transport for individual or multiple swash events is very difficult using sediment traps and suspended sediment measurements. However, the high flow velocities and movement of ridges of sediment over the beach face can lead to bed elevation changes of several centimeters per swash. *Baldock et al.* [2006] measured these rapid changes in bed elevation using pressure transducers buried across the SZ. The transducers enable interswash measurements of changes in the elevation of the saturated sand surface and hence the bed level changes over time (Figure 10). In this example, a gradual erosion trend is punctuated by short episodes of significant local accretion. However, while data from a single point provide an indication of the dynamic behavior of the bed level, they do not provide much useful information in terms of describing the overall sediment flux.

[36] For example, Figure 11 shows a plot of bed elevation change per swash event versus the maximum swash depth for each swash event observed at the same point. The data show no correlation between the maximum swash depth and the local erosion or accretion of the bed; that is, for these data, the magnitude of the swash event has little bearing on the net deposition or erosion of the sediment at that location. This is because single-point measurements provide no information on the motion of sediment advected into, across, or out of the SZ.

[37] To address this, *Baldock et al.* [2006] obtained measurements of bed elevation change per swash from multiple cross-shore locations. This enables the cross-shore variation in the net total sediment flux to be derived across the full SZ for either individual or multiple swash events (Figure 12). The cross-shore distribution of the total net sediment transport shown in Figure 12 is consistent with the numerical calculations presented by *Pritchard and Hogg* [2005], where the advection of sediment into the SZ is shown to be an important factor in the net erosion or accretion of the beach. Data of this form will assist the development of more complete models that balance the uprush/backwash sediment fluxes by incorporating the advection of presuspended sediment into the SZ [*Pritchard and Hogg*, 2005]. *Pritchard and Hogg* [2005] also showed that the sediment entrained in the incident bore (see Figure 13) is likely to play an important role in the net sediment balance in the SZ. However, in this respect, the SM63

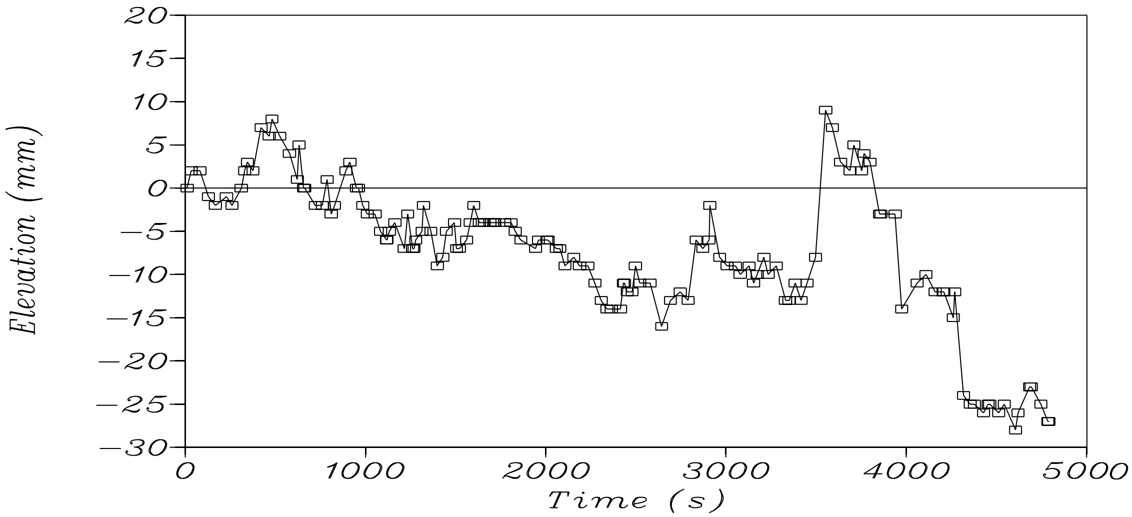

Figure 10. Bed elevation following individual swash events obtained from a pressure sensor buried a few centimeters below the sand surface on a natural beach with grain size 0.2 mm. Gradual erosion of the beach face is interrupted by shorter episodes of accretion.

model predicts that sediment is advected into the SZ from a very narrow region of the surf zone, approximately 1/16 of the runup length [*Pritchard and Hogg*, 2005]. However, measurements in both the field and laboratory suggest that the potential length of this region is between 1/5 and 1/3 of the runup length [*Baldock et al.*, 2007a], which will give a corresponding increase in the contribution of presuspended sediment to the net sediment balance in the SZ.

[38] The longshore flux of mass and momentum induced by oblique wave runup influences circulation patterns in the inner surf zone and leads to longshore variations in sediment flux. A wide range of longshore spatial scales has been observed in SZ shoreline motions [*Holland and Holman*, 1999], which can be expected to be mirrored in the morphologic scales (e.g., beach cusps and embayments). However, a consensus has yet to be reached on whether edge waves or oblique short waves are the primary forcing mechanism [*Coco et al.*, 2003]. The runup from oblique short-crested wave groups will similarly induce longshore variations in the shoreline motion, the cross-shore and longshore flows, and hence the sediment fluxes across the swash-surf zone boundary. In this case, strong hydrodynamic-morphodynamic feedback is possible since the nearshore wave group structure is determined by the bathymetry in the surf zone.

[39] Over longer durations (minutes and hours as opposed to individual swash events), the complexity and difficulty of predicting morphological evolution in the SZ is illustrated by the cyclic patterns of alternating accretion and erosion on the beach face during flood and ebb tides [*Grant*, 1948; *Duncan*, 1964]. While these may be linked to changes in sediment transport induced by tidally varying infiltration/exfiltration of water across the beach face as suggested by *Grant* [1948], some recent observations show

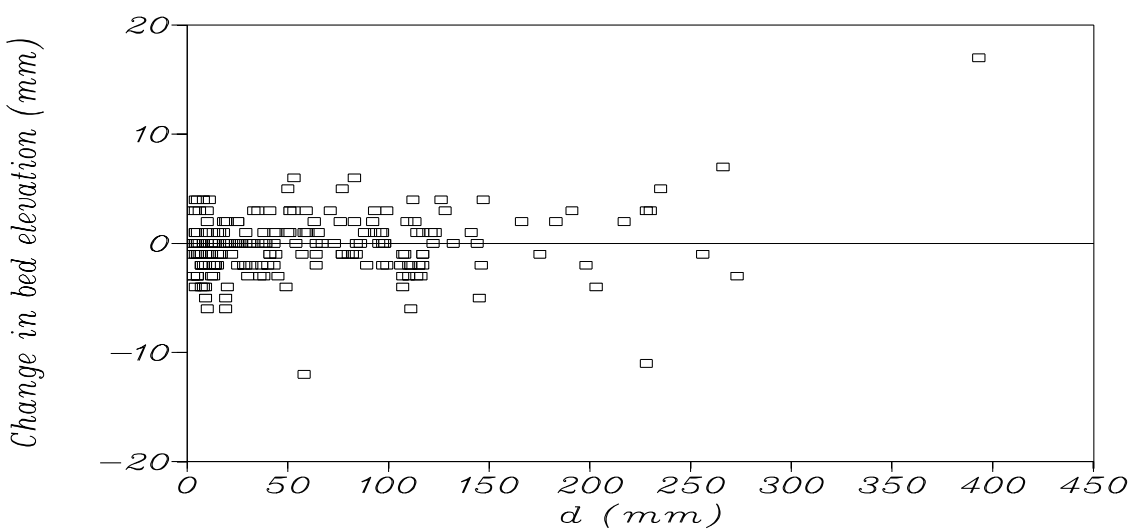

Figure 11. Bed elevation change per swash versus maximum swash depth, *d*. Data are obtained from a pressure sensor buried a few centimeters below the sand surface on a natural beach with grain size 0.2 mm.

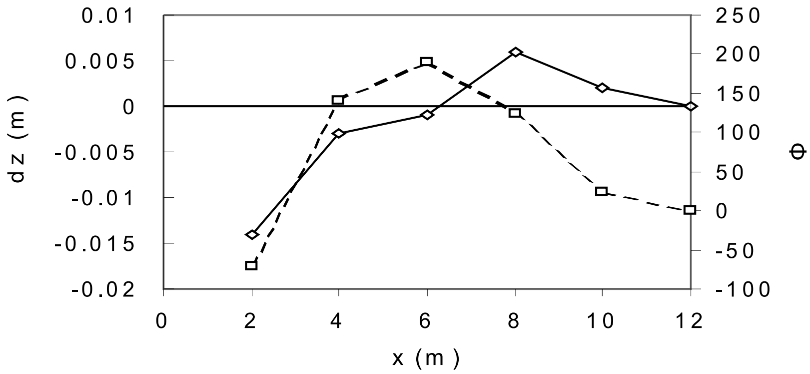

Figure 12. Cross-shore variation in sand level changes, dz (solid line with diamonds), and nondimensional total net sediment flux, ϕ (dashed line with boxes), over a single swash event. Here $x = 0$ corresponds to x_l as defined on Figures 2 and 3. Grain size $d_{50} = 0.525$ mm. Adapted from *Baldock et al.* [2006], with permission from ASCE.

more complex behavior [*Weir et al.*, 2006], with accretion seaward of the groundwater exit point on the ebb tide (Figure 14) and little overall consistency with the Grant hypothesis, which suggests accretion on the flood tide (high infiltration) and erosion on the ebb tide (high exfiltration). For these data, the boundary between swash erosion/accretion corresponds quite closely to the landward limit of swash interactions Z_{int}. This suggests that the increased turbulence and additional suspension of sediment by swash-swash interaction plays a role in the net transport. Of further interest is the temporal variation in the runup distribution between flood and ebb tide (indicated by the elevation exceeded by 50% and 2% of the waves, $Z_{50\%}$ and $Z_{2\%}$, respectively) between flood and ebb tide. The vertical swash excursion (i.e., the runup above the maximum rundown position, $Z_{0\%}$) is significantly greater on the flood tide than on the ebb tide, indicating different SZ conditions at the same surf zone water levels. This difference appears to have an influence on the morphological response; on the flood tide, erosion and accretion occur at elevations above

Figure 13. Presuspended sediment in an incident bore just prior to collapse at the shoreline. The orange string lines are horizontal and spaced 5 cm apart. The vertical rods are 1 m apart. The water surface dips seaward until the toe of the incident bore, indicating that the total acceleration is negative (seaward) until the bore passes.

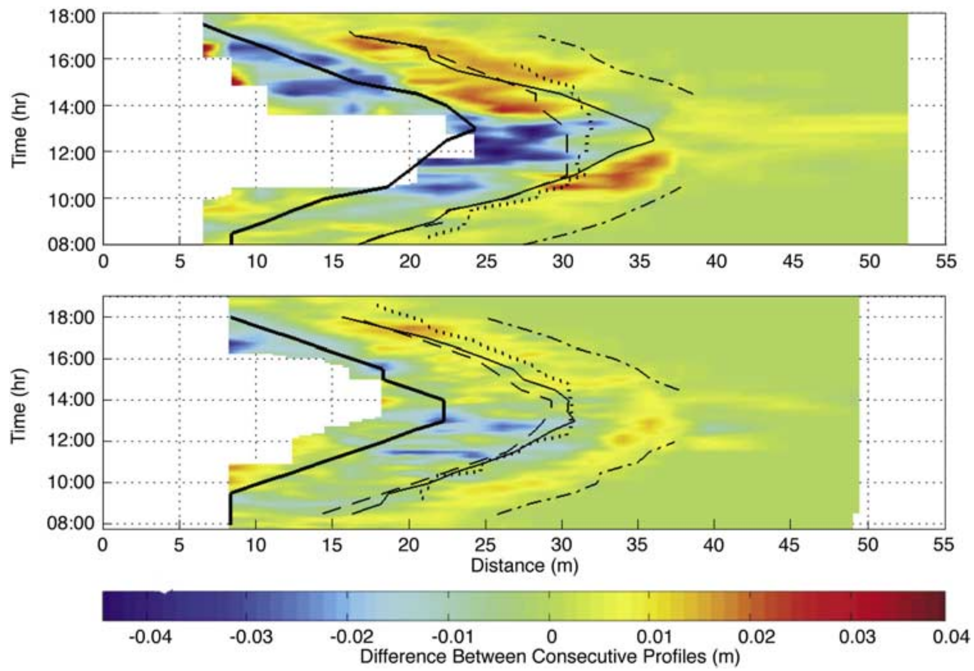

Figure 14. Color mapping of bed elevation change between consecutive beach profiles measured quarter hourly, plotted as a function of time and cross-shore distance. Color bar indicates magnitude of bed elevation changes. The locations of the maximum run-down position, Z_0 (thick solid line), $Z_{50\%}$ (thin solid line), $Z_{2\%}$ (dash-dotted line), and Z_{int} (dashed line) and upper limit of the groundwater effluent zone (dotted line) are also shown. Adapted from *Weir et al.* [2006], reprinted with permission from Elsevier.

$Z_{0\%}$ and $Z_{50\%}$, respectively, while on the ebb tide, erosion and accretion occur along these locations. Further work is required to link these patterns with inner surf zone wave conditions and to determine why the runup distribution is asymmetric with respect to the tidal water levels.

3. MODELING THE SZ: PACKING UP SCALES

[40] It is clear that SZ dynamics strongly influence the surf zone hydromorphodynamics. However, SZ dynamics are often neglected in computations of coastal flows, be they carried out at a wave-resolving level (i.e., time domain models) or at a wave-averaging level (i.e., circulation models).

[41] Simplified shoreline boundary conditions (SBCs) are often used such that either perfect absorption [*Wei et al.*, 1999; *Johnson et al.*, 2005] or perfect reflection [*Bradford*, 2005] is enforced at the inshore boundary of the computational domain. Both of them are clearly incorrect as they prescribe the wrong magnitude and shape of LFWs radiating out to sea. In the former case, generally obtained through a sponge layer, all incoming waves are lost. However, for perfect reflection, usually obtained by fitting a rigid wall at the still water shoreline, all incoming LFWs are reflected at one single point, and no generation or modification of LFWs can occur within such infinitesimal SZ. A third type of SBC, i.e., a SZ condition, is required. To clarify the importance of the SBC, Figure 7 illustrates the main difference in the pattern/intensity of seaward propagating LFWs induced by groups of wind waves either incoming onto a wall (left plots) or allowed to generate a SZ (right plots). Both the magnitude of the outgoing waves (thick lines in the lower plots) and the shape of the LFWs is altered (note the different magnification factors in Figure 7). Future nearshore circulation models therefore should include appropriate SBCs. However, implementation of swash SBCs is not an easy task in view of the range of scales to be bridged, as discussed in section 3.3.

3.1. Small Scales: Turbulence and Sediment Pickup

[42] Turbulence in the inner surf and SZ influences the bottom boundary layer and results in the pickup and maintenance of sediment suspensions [*Kobayashi and Johnson*, 2001]. During the uprush, turbulence generated and advected into the SZ from the incident bore dominates over wall-generated turbulence and vice versa during the backwash [*Petti and Longo*, 2001; *Cowen et al.*, 2003]. However, insufficient data exist to quantify either effect for use within a sediment-modeling framework.

[43] Recent experimental studies have examined the role played by externally generated turbulence (grid turbulence) on oscillatory wave boundary layers [*Fredsoe et al.*, 2003; *Hsu and Raubenheimer*, 2006]. It has been found that (1) externally generated turbulence penetrates the bed boundary layer, giving rise to an increase in both the mean and RMS values of the bed shear stress when compared to the undisturbed case, and (2) the phase lead of the shear stress over the flow velocity decreases and the friction coefficient increases with increasing turbulence intensity.

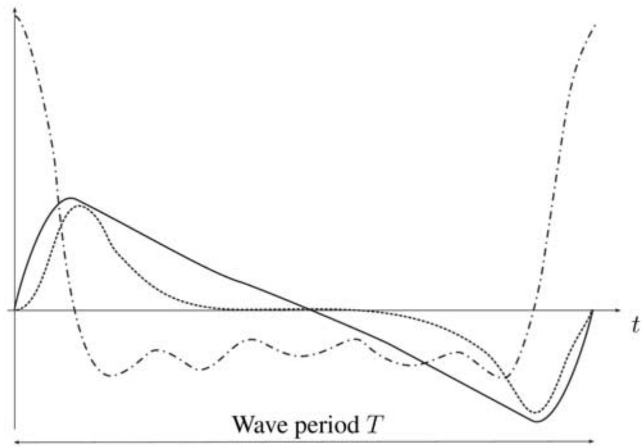

Figure 15. Near-bed flow variables under sawtooth waves: free-stream velocity u (solid line), velocity cubed u^3 (dashed line), and flow acceleration du/dt (dashed-dotted line).

These effects, if applicable within the SZ, are likely to contribute to some of the asymmetry between uprush and backwash friction factors. For example, the turbulence stirring produced during the uprush by collapsing bores is absent during the backwash phase [*Puleo et al.*, 2000].

[44] In the inner surf zone, the waves are sawtooth-shaped, but the onshore-offshore velocity is quite symmetric. The small velocity asymmetry in the free streamflow leads to vanishing sediment transport rates q over a wave cycle for all velocity-based formulae of the type $q \propto \langle u^3 \rangle$ [e.g., *King*, 1991] (see also Figure 15). However, turbulence effects and the acceleration of the external flow du/dt lead to conditions such that for a given free-stream velocity, a stronger bed shear stress occurs during the rapidly accelerating flow because of passage of the bore front than during the more gradually accelerating seaward flow following flow reversal. Recently, various models of bed shear stress τ generated by an arbitrary free-stream velocity u have been proposed [*Drake and Calantoni*, 2001; *Nielsen*, 2002] and which lead to nonvanishing sediment transport rates under sawtooth waves with zero velocity asymmetry in the free-stream flow. These forms of models are essential if the modeling of the shoreward transport of sediment from the inner surf zone into the SZ is to be successful. While this boundary layer thinning or thickening is often attributed to the local acceleration, it is more correct to attribute it to the influence of the pressure gradient imposed across the boundary layer. Consequently, it is the pressure gradient, or total acceleration, that is important.

[45] Swash flows, in contrast, differ in a number ways that are important in sediment transport modeling. First, the local ($\partial u/\partial t$) and total ($\partial u/\partial t + u\partial u/\partial x$) horizontal fluid accelerations are predominantly directed seaward, with some strong, but limited-duration, shoreward directed advective acceleration occurring close to the run-down position [*Hughes and Baldock*, 2004]. Consequently, *Baldock et al.* [2005] suggest caution in applying sediment transport models that incorporate acceleration effects, since the acceleration is seaward and this actually reduces the magnitude of the calculated transport rates. Second, for natural beaches, the interaction between the bore turbulence and the high sediment concentrations is important and can be expected to modify the turbulence structure in comparison to a fixed bed. In particular, high concentrations of sediment can lead to density gradients similar to those occurring in stratified flows, hence the unavoidable reduction of vertical turbulence and flow mixing. At these scales, the most important two factors in terms of overall SZ sediment dynamics appear to be the quantity of presuspended sediment in the turbulent bore front (see Figure 13) and the settling rate of the suspended sediment in the SZ. The former plays a strong role in the overall net sediment transport within the swash, while the latter has a more subtle effect in modifying the cross-shore distribution of the sediment flux [*Pritchard and Hogg*, 2005]. In terms of modeling approaches, both effects appear relatively straightforward to specify as SBCs. For the presuspended load, a fixed or time-varying suspended sediment concentration can be specified at the boundary. The effects of turbulence and hindered settling can be formulated in terms of a modified sediment fall velocity, the effects of which can be integrated over the SZ and applied as a SBC. Very advanced semi-analytical approaches are becoming available for an accurate description of the coupling between the hydrodynamic flows and both the bottom [*Fraccarollo and Capart*, 2002] and suspended [*Pritchard and Hogg*, 2005] sediment transport. These seem to be excellent tools for both implementation and evaluation of numerical solvers for the SZ hydromorphodynamics.

3.2. Intermediate Scales: Waves and Sediment Suspension/Transport

[46] The SZ is presently neglected entirely in most applied large-scale coastal hydromorphodynamic modeling suites. Furthermore, long waves and a full representation of random waves are also presently ignored throughout the model domain in such large-scale morphodynamic models. While these are, perhaps, reasonable simplifications in the surf zone, they are much less so in the SZ, since the LFWs and wave grouping effects are magnified in the SZ as discussed in section 2.3. Modeling of the SZ hydrodynamics and morphological evolution can be performed in the same way as for waves by formulating time-integrated descriptions of the cross-shore variation in flow velocity and sediment flux for individual swash events [*Alsina et al.*, 2005; *Pritchard and Hogg*, 2005]. However, instead of choosing a single representative swash based on a representative wave height and wave period, future broad-scale modeling should follow a deterministic-probabilistic approach to account for random wave runup. Thus, time-integrated net transport rates are required for a distribution of bore heights at the shoreline or, equivalently, a distribution of runup elevations.

[47] For random waves, the runup varies for individual bores in the probability distribution. In addition, the prob-

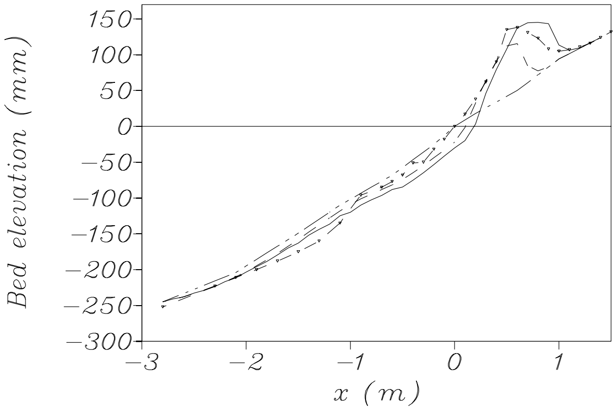

Figure 16. Model-data comparisons for an accreting laboratory-scale beach: initial profile (dashed-double-dotted line), measured profile (dashed line with triangles), probabilistic model (solid line), and monochromatic model (dashed line). Grain size d_{50} = 1.5 mm; wave period is 1.5 s; wave height is 0.09 m; ξ = 0.55. Adapted from *Baldock et al.* [2007a], with permission from ASCE.

ability of occurrence of each bore height varies. Hence, a different net cross-shore sediment transport pattern results in comparison to monochromatic waves. Furthermore, determining the swash sediment transport with a single representative RMS bore height underestimates the runup and morphological evolution of the upper beach and does not account for the morphodynamic smoothing effect of varying swash excursions. Observed probability density functions for inner surf zone bore heights and swash runup maxima vary between a normal distribution and a Rayleigh distribution, appropriate for broadbanded and narrowbanded runup processes, respectively [*Battjes*, 1971; *Nielsen and Hanslow*, 1991; *Holland and Holman*, 1993]. Such probability distributions can also be used to describe the water depths in the SZ [*Kobayashi et al.*, 1998]. Therefore, incorporating random wave swash in a parametric model framework can be achieved by calculating the sediment transport for a Rayleigh-distributed range of bore heights and by weighting the net transport according to the probability of different bore heights occurring. Consequently, given any monochromatic wave net cross-shore transport function, $q_m(x, H)$, the resulting total random wave net swash transport per wave, $q_r(x, H_{\mathrm{RMS}})$, for a Rayleigh probability density function becomes

$$q_r(x, H_{\mathrm{RMS}}) = \sum_{H_{\min}/H_{\mathrm{RMS}}}^{H_{\max}/H_{\mathrm{RMS}}} q(x, H)\frac{2H}{H_{\mathrm{RMS}}} \cdot \exp\left[-\left(\frac{H}{H_{\mathrm{RMS}}}\right)^2\right]\Delta\left(\frac{H}{H_{\mathrm{RMS}}}\right), \tag{7}$$

where (H/H_{RMS}) is the bin width used in the summation. This approach is computationally cheap and can be readily incorporated within existing parametric model routines. For example, Figure 16 shows the measured and predicted morphodynamic evolution of an initially plane mobile bed laboratory beach model under random wave conditions using both a monochromatic swash model and the probabilistic model described in (7) [*Baldock et al.*, 2007a]. The probabilistic model results in sediment transport across a wider SZ, and this is particularly important for describing sediment deposition near the runup limit and the growth of beach berms.

[48] The time-integrated deterministic-probabilistic transport rates can then be imposed at the appropriate broad-scale morphologic time step. The influence of long waves in sweeping short waves across the beach face could be incorporated in a similar manner, with the long waves either uncorrelated or correlated with the incident bores at the shoreline. This correlation depends on the LFWs generation mechanisms farther offshore. For small ξ, the correlation is probably negative or weakly positive [*Battjes et al.*, 2004]; for higher ξ (which for the same beach slope corresponds to steeper storm waves), the correlation is more likely to be stronger and positive [*Baldock*, 2006]. Stronger positive correlation between the LFWs and short waves is likely to result in more constructive interference between LFWs and short waves, with a large volume of water temporarily stored on the beach face when a long-wave uprush and a group of large short waves coincide. The subsequent withdrawal of the shoreline tends to be rapid, with a corresponding increase in backwash flow velocities and the potential for greater associated offshore sediment transport.

[49] Morphodynamic feedback between the SZ and surf zone has long been recognized, for example, the classical erosion of the shoreface during storms that results in sediment deposition on a longshore bar. The longshore bar then induces more wave breaking and energy dissipation in the surf zone, reducing the rate of beach face erosion. However, the role of the SZ in influencing surf zone morphology during beach recovery, and particularly onshore bar migration, does not appear to have been considered in great detail. Recent analyses [*Baldock et al.*, 2007a] revealed that extensive swash overtopping of a low beach berm was associated with rapid growth of the beach berm but with little change in beach gradient and little seaward migration of the berm crest. Consequently, the berm was acting as a sediment sink, with the surf zone acting as a strong sediment source. Similarly, a strong landward transport in the surf zone was observed during swash overtopping on a laboratory-scale beach [*Baldock et al.*, 2005]. In both cases, the influence of the reduced backwash flows appeared to have a strong influence on the shoreward transport of sediment in the surf zone. Recent small-scale experiments carried out to investigate this morphological swash-surf zone feedback are discussed by *Baldock et al.* [2007b], and an example is illustrated in Figure 17.

3.3. Large Scales: Low-Frequency Waves, Currents, and Morphodynamics

[50] The coastal hydromorphodynamic evolution at the larger scales is studied by means of models that average the wave dynamics (wave-averaged models). Although they are well developed, wave-averaged models use some assumptions that limit their capabilities of reproducing natural flow

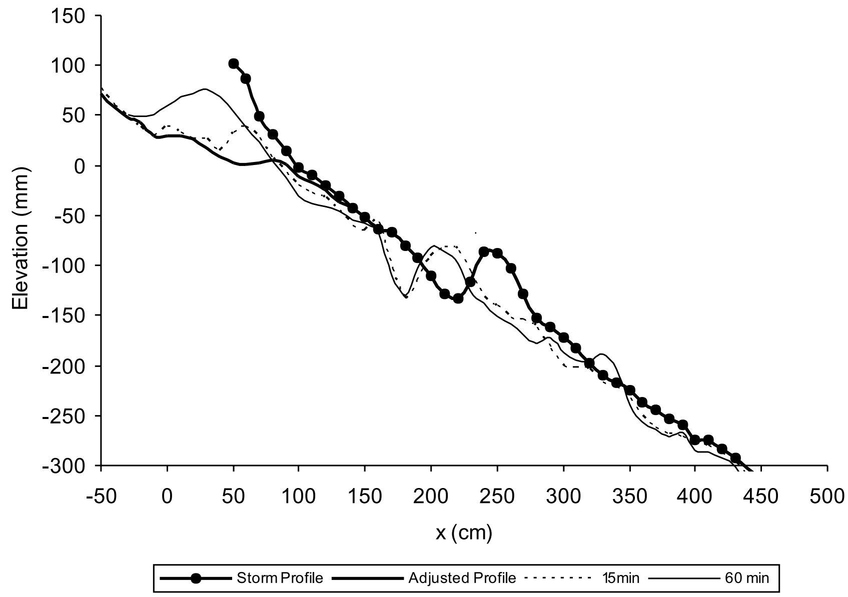

Figure 17. Swash-surf zone morphodynamic feedback. An equilibrium barred beach profile was reshaped with a smaller gradient in the SZ and then subject to milder wave conditions. Lines show beach profile at subsequent times indicated. Berm growth and enhanced onshore movement of a longshore bar was triggered by the flattening of the beach profile in the SZ. A control beach, subject to the same wave conditions and with no adjustment to the SZ profile, showed little subsequent change in the SZ morphology and slower onshore bar migration. Adapted from *Baldock et al.* [2007b], reprinted with permission from Coastal Education and Research Foundation, Allen Press Publishing Services.

conditions. One of the most crucial shortcomings concerns the treatment of the boundary between the wet and dry domains. Since such a boundary is taken as the location where the mean total water depth vanishes ($\overline{d} = 0$), both theoretical and practical problems arise. From the theoretical point of view, since during a wave cycle $\overline{d} = 0$ only occurs at the maximum runup location, flow integration would occur also during periods of local dry conditions. Using wave-averaged models, in which short waves force the mean flow only through radiation stresses computed within this "artificial mean swash," also makes it impossible to properly account for the interaction between short waves and long waves, fundamental for a correct energy partitioning of the nearshore flows [*Mase*, 1995]. It is particularly worrying that longshore sediment transport is not adequately represented by models that neglect SZ hydrodynamics. Such sediment transport within the SZ, forced by drift motions that result in a "zigzag transport" [*Brocchini*, 1997], is now acknowledged as one of the fundamental mechanisms for beach morphology evolution.

[51] Analysis of different definitions for the mean shoreline made by *Brocchini and Peregrine* [1996] has revealed that such a mean interface cannot be uniquely defined. However, problems can be overcome if the boundary between wet and dry is taken as the envelope of the rundown positions (line x_l of Figure 18), since flow properties can be unambiguously defined only within the wet region.

[52] The integral model proposed by *Brocchini and Peregrine* [1996] has recently been used as the basis for the definition of suitable SBC for wave-averaged models [*Brocchini and Bellotti*, 2002; *Bellotti et al.*, 2003; *Bellotti and Brocchini*, 2005; *Antuono et al.*, 2006]. The main outcome of such analysis is summarized by the following local (i.e., at the mean shoreline x_l) conditions for the mean water depth $\overline{d}$, the mean onshore velocity W, the longshore SZ water drift velocity $\overline{u}$, and the mean shoreline position x_l:

$$\frac{dx_l}{dt} \approx \overline{u} - \frac{4C_V}{\gamma}\frac{dH}{dt},$$
$$\overline{d} \approx \frac{H}{2}, \overline{u} \approx \mathcal{R}_+ - \sqrt{2gH},$$
$$W \approx \left[C_1 + \frac{C_2}{C_f}\hat{T}\right]\sin(\theta)\sqrt{gH}. \tag{8}$$

These can be readily interpreted as follows:

[53] 1. The motion of the mean shoreline depends on the local mean velocity $\overline{u}$ and on the rate of change of the water volume stored in the SZ (which is proportional through C_V to dH/dt).

[54] 2. At the mean shoreline, the mean water depth can be computed by taking the incident bore as a triangular water wedge (see also Figure 19) of height H and length $\sqrt{gH}T$ [*Bellotti et al.*, 2003].

[55] 3. The local onshore velocity depends on the local shallow water velocity $\overline{u}$ and on the information $\mathcal{R}_+$ carried along positive characteristics from the offshore region toward the shoreline.

[56] 4. The drift velocity W depends on the expected fraction of the local shallow water velocity (i.e., $\sin(\theta)\sqrt{gH}$) through two terms. The first term (C_1) accounts for short-wave interactions and purely nonbreaking, nonlinear contributions, and the second term, proportional to the swash

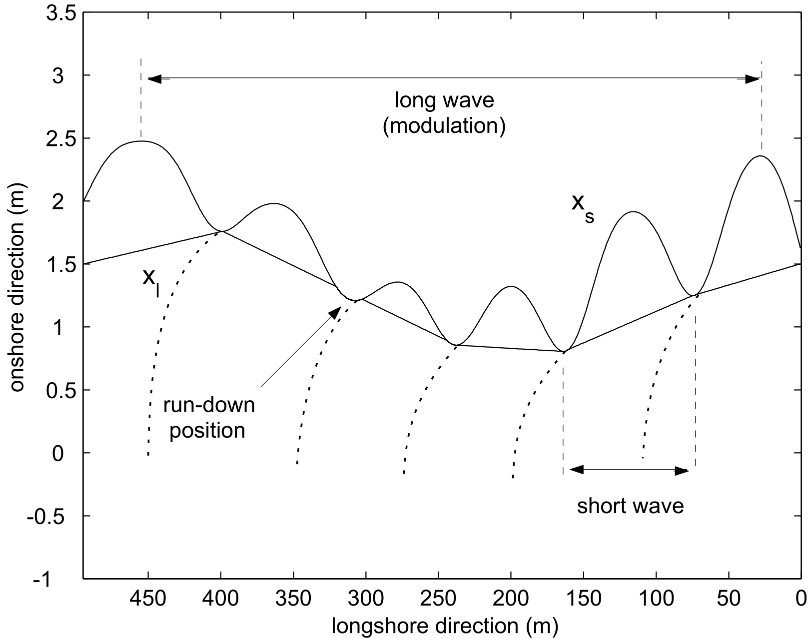

Figure 18. Sketch at a given time of the flow evolution of the SZ induced by bimodal waves propagating over a uniformly sloping beach of slope γ and with friction coefficient C_f. The instantaneous, local shoreline (x_s), the envelope of the run-down positions (x_l), and an indication of the bore paths (dash-dotted lines) are illustrated. Adapted from *Antuono et al.* [2006], reprinted with permission from Cambridge University Press.

interaction parameter $\hat{T}$, models forcing from breaking waves [*Antuono et al.*, 2006].

[57] These compact SBC naturally account for the interactions of long waves and short waves near the shoreline and represent a suitable novel method for taking into account SZ flows in wave-averaged models. Moreover, being based on an integral approach [*Brocchini and Peregrine*, 1996], their accuracy in representing the SZ dynamics improves as a function of the accuracy with which parameterizations for the integral properties are made.

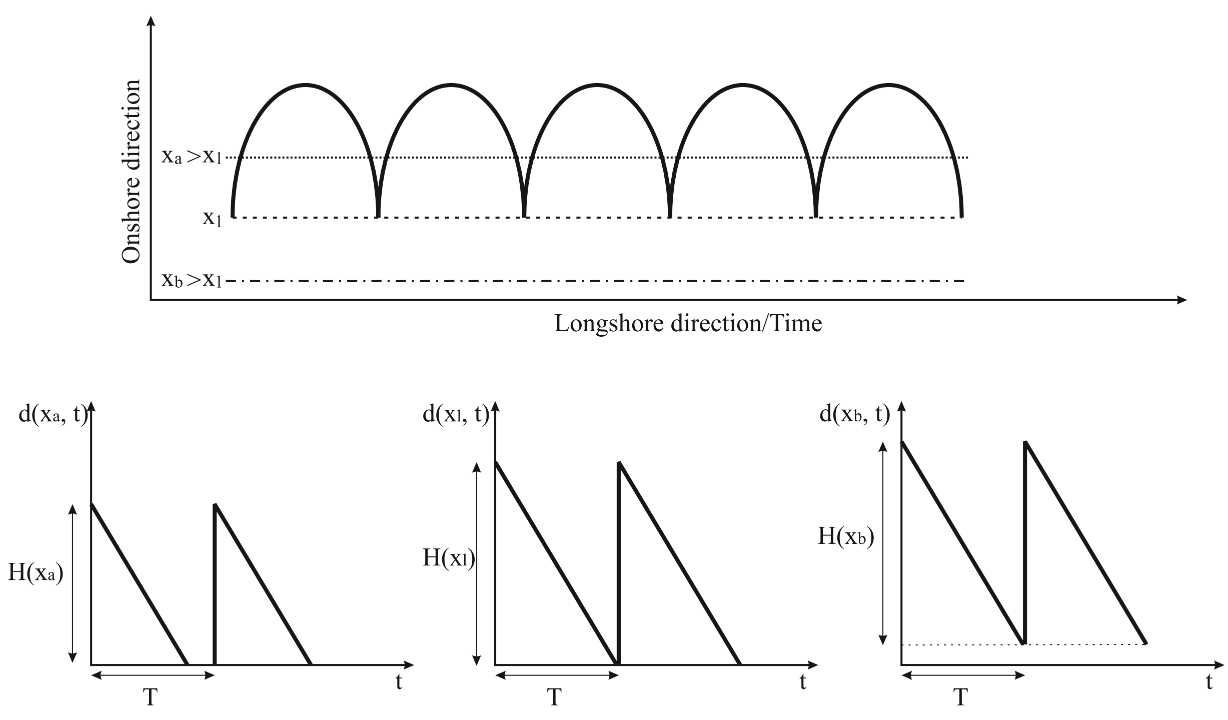

Figure 19. Sketch of the "trapezium model" of *Bellotti et al.* [2003] for various onshore beach locations. The time series of the water depth d are shown for regular waves shoreward of the run-down location ($x_a > x_l$), at the run-down location (x_l), and seaward of the run-down location ($x_b < x_l$).

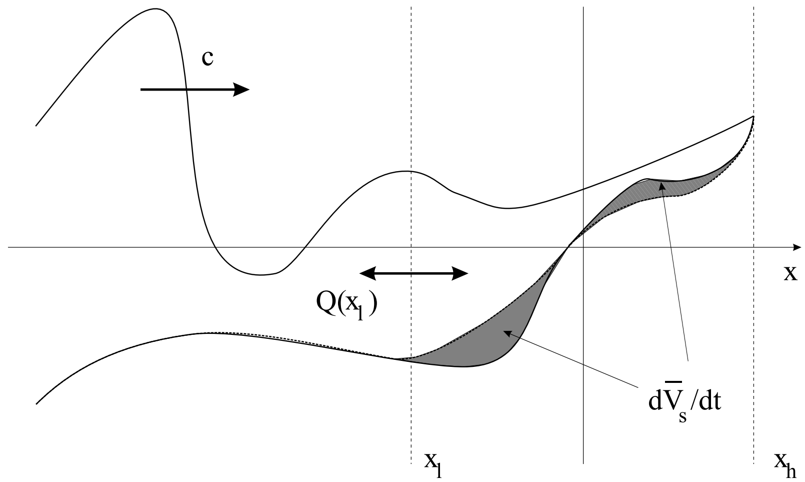

Figure 20. Illustration of flow variables used in the simplified morphodynamics condition (9). The shaded area shows the rate of change of sediment volume in the SZ computed as the difference between two subsequent bed configurations.

[58] One simple, though important, use of these SBCs is their employment as a benchmark for validation of nearshore circulation solvers. This has recently been attempted by R. Briganti and Q. Chen (Effects of shoreline boundary conditions in Boussinesq modeling of nearshore circulation, submitted to *Coastal Engineering*, 2007), who found that the available techniques used to represent the motion of the shoreline within Boussinesq-type models lead to a substantial underestimation of the longshore drift. Such underestimation is likely to strongly affect the predictions of longshore sediment motion within the SZ [*Bodge*, 1989; *Elfrink and Baldock*, 2002].

[59] The potentials of the integral model are fully exploited when defining SBCs for hydromorphodynamic solvers, i.e., when a sediment transport dynamical equation is coupled to the hydrodynamic equations (NSWE). A first attempt has already been made with some success [*Casale et al.*, 2002]. A boundary condition, based on a local and instantaneous mass conservation equation, has been derived and which is coupled with the hydrodynamic SBCs (8). This condition is derived from an Exner-type equation by integration over the SZ width and averaging over the short waves. Approximations of boundary contributions at both x_l and x_h lead to the simple expression

$$(1-p)\frac{d\overline{V}_s}{dt} \approx \overline{Q}(x_l, t). \quad (9)$$

Here p is the bed porosity, $\overline{Q}(x_l,\ t)$ is the mean (wave averaged) sediment flow rate crossing $x = x_l$, and $\overline{V_s}$ is the mean volume of sediment within the SZ, i.e., between $x_l < x < x_h$ and above a given horizontal reference level (see also Figure 20).

[60] Small-scale (model-to-prototype geometric ratio of 1:10) laboratory experiments revealed a good balancing of equation (9), the order of magnitude of both sides of the equation being the same. However, they also showed that (1) more analyses are required to safely rule out important boundary effects at x_l and x_h and (2) accurate measurements of the sediment flow rate $\overline{Q}(x_l)$, which are not easy to obtain, are essential for assessing the exact balance of equation (9). Hence, further experiments are needed both at laboratory and at prototype scale, the latter to minimize scale effects. In any case, coupling of the hydrodynamics conditions (8) and the morphodynamic condition (9) seems rather straightforward, both being of hyperbolic nature, which can be easily cast in vectorial form suitable for application of modern solution techniques like volume of fluid Godunov-type solvers [*Toro*, 2001].

[61] The approach that seems most useful to provide the morphodynamics SBCs is that for which $d\overline{V}_s/dt$ is parameterized in terms of mean flow (wave height) and sediment variables [e.g., *Brocchini and Bellotti*, 2002], so that the sediment concentration at x_l can be obtained as a boundary value for the hydromorphodynamic solver. The rate of change of the volume of sediment in the swash zone, $d\overline{V}_s/dt$, can be obtained in the field using the approach of *Baldock et al.* [2006] described in section 2.4.

4. FUTURE RESEARCH

[62] The review above has attempted to highlight recent progress in describing the hydrodynamics, sediment dynamics, and morphodynamics within the SZ. While recent progress is promising, the prediction of the correct net sediment transport on the beach face remains a formidable challenge. Future improvements will come from a range of analytical, numerical, and experimental data, and the latter will require both field and laboratory studies.

[63] Very recent fundamental studies on the overall structure of the boundary value problem for the NSWE [*Antuono and Brocchini*, 2007] will provide the solid theoretical foundations for investigating the SZ hydrodynamics forced by both periodic and pulse-like waves

irrespective of the limitations introduced by the solution of the initial value problem (this being the standard practice until now).

[64] The work of *Pritchard and Hogg* [2005] provides an important platform for further analytical modeling of swash processes, particularly for models working in a Lagrangian framework. Working in this reference frame removes one major difficulty, notably that of the intermittency of the flow. Consequently, models based on continuous descriptions of the flow, including Fourier transforms and their derivatives, can provide useful solution techniques. Furthermore, discontinuities in the boundary conditions (e.g., dry/wet regions) can be avoided. Models in a Lagrangian framework also enable the inclusion of advected sediment and solutions of the advection-diffusion equation in sediment dynamics models [*Alsina et al.*, 2005], and further work is required using this approach.

[65] In terms of numerical modeling, finite volume solvers, direct Navier-Stokes solvers, and Reynolds-averaged Navier-Stokes solvers appear able to provide accurate and detailed descriptions of SZ hydrodynamics. These will be useful in providing the flow velocities, and possibly descriptions of the turbulence, in regions of the flow that are beyond the present measurement capability of laboratory and field instrumentation. In conjunction with recent data providing improved descriptions of the bed shear stress under swash flows, this provides an opportunity to formulate and test improved boundary layer models for the SZ. The influence of adverse and favorable pressure gradients on boundary layer development during the uprush and the backwash, respectively, remains to be investigated.

[66] Measurements of the total net transport as reported in Figure 12 now enable a description of the cross-shore gradients in sediment transport for single and multiple swash events in the field. Further data are required, and this will provide a robust test of sediment transport and morphological models. In conjunction, further data from traditional instrumentation are required to provide detailed descriptions of the suspended sediment load. At present, accurate measurements of the sheet flow bed load have yet to be performed, but a combination of the total load and suspended load may enable indirect estimates of this. However, again, spatially dense data are required to determine gradients in the sediment flux.

[67] Finally, while the importance of long waves has long been recognized in terms of the SZ hydrodynamics and shoreline motion, most applied models neglect the randomness of the incident wavefield and both the free and bound long waves associated with wave groups. Furthermore, the influence of long waves and wave groups on the beach face morphodynamics has yet to be investigated in great detail but appears significant [*Baldock et al.*, 2007b]. Long-wave effects may be direct and indirect, the latter arising from the long waves sweeping short waves across the beach, and both are probably dependent on ξ and the correlation between the short waves and long waves. The complexity of the problem in the field, combined with the requirement to obtain data over large spatial extents, suggests that short-term progress in this area will be the result of laboratory investigations.

[68] **ACKNOWLEDGMENTS.** The authors gratefully acknowledge the contributions of their coauthors on papers cited herein, particularly Matteo Antuono, Renata Archetti, Matt Barnes, Giorgio Bellotti, Giovanna Grosso, Michael Hughes, and Felicia Weir.

[69] The Editor responsible for this paper was Henk Dijkstra. He thanks two anonymous technical reviewers and one anonymous cross-disciplinary reviewer.

REFERENCES

Alsina, J., T. Baldock, M. Hughes, F. Weir, and J. Sierra (2005), Sediment transport numerical modelling in the swash zone, paper presented at the Coastal Sediments 2007, Am. Soc. of Civ. Eng., New Orleans, La.

Antuono, M., and M. Brocchini (2007), The boundary value problem for the nonlinear shallow water equations, *Stud. Appl. Math.*, *119*(1), 73–93.

Antuono, M., M. Brocchini, and G. Grosso (2006), Integral flow properties of the swash zone and averaging. part 3. The longshore flow, *J. Fluid Mech.*, *573*, 399–415.

Baldock, T. E. (2005), Long wave generation by the shoaling and breaking of transient wave groups on a beach, *Proc. R. Soc., Ser. A*, *462*, 1853–1876.

Baldock, T. E., and P. Holmes (1999), Simulation and prediction of swash oscillations on a steep beach, *Coastal Eng.*, *36*, 219–242.

Baldock, T. E., and M. G. Hughes (2006), Field observations of instantaneous water slopes and horizontal pressure gradients in the swash-zone, *Cont. Shelf Res.*, *26*, 574–588.

Baldock, T. E., and D. A. Huntley (2002), Long wave forcing by the breaking of random gravity waves on a beach, *Proc. R. Soc. London, Ser. A*, *458*, 2177–2201.

Baldock, T. E., P. Holmes, and D. P. Horn (1997), Low frequency swash motion induced by wave grouping, *Coastal Eng.*, *32*, 197–222.

Baldock, T. E., M. G. Hughes, K. Day, and J. Louys (2005), Swash overtopping and sediment overwash on a truncated beach, *Coastal Eng.*, *52*, 633–645.

Baldock, T. E., M. P. Barnes, and M. G. Hughes (2006), Field observations of instantaneous cross-shore free surface profiles and flow depths in the swash zone, in *Coastal Dynamics 2005-State of the Practice* [CD-ROM], edited by A. Sanchez-Arcilla, Am. Soc. of Civ. Eng., Reston, Va.

Baldock, T. E., P. K. Son, P. Manoonvoravong, M. P. Barnes, and J. M. Alsina (2007a), Probabilistic-deterministic modelling of swash zone morphology, in *Coastal Sediments 2007*, edited by N. C. Kraus and J. D. Rosati, pp. 272–285, Am. Soc. of Civ. Eng., Reston, Va.

Baldock, T. E., P. Manoonvoravong, and K. S. Pham (2007b), Beachface morphology and surf beat sediment transport in laboratory scale surf and swash zones, *J. Coastal Res.*, *SI50*, 631–635.

Barnes, M., and T. Baldock (2007), Direct bed shear stress measurements in laboratory swash, *J. Coastal Res.*, *SI50*, 641–645.

Barnes, T. (1996), The generation of low frequency waves on beaches, doctoral thesis, Univ. of Bristol, Bristol, U. K.

Battjes, J. (1971), Run up distributions of waves breaking on slopes, *J. Waterw. Harbors Coastal Eng. Div. Am. Soc. Civ. Eng.*, *97*(WW1), 91–114.

Battjes, J., H. Bakkenes, T. Janssen, and A. van Dongeren (2004), Shoaling of subharmonic gravity waves, *J. Geophys. Res.*, *109*, C02009, doi:10.1029/2003JC001863.

Bellotti, G., and M. Brocchini (2005), Swash zone boundary conditions for long wave models, *Coastal Eng.*, *52*, 971–976.

Bellotti, G., R. Archetti, and M. Brocchini (2003), Experimental validation of mean swash zone boundary conditions, *J. Geophys. Res.*, *108*(C8), 3250, doi:10.1029/2002JC001510.

Boak, E., and I. Turner (2005), Shoreline definition and detection: A review, *J. Coastal Res.*, *21*, 688–703.

Bodge, K. (1989), A literature review of the distribution of longshore sediment transport across the surf zone, *J. Coastal Res.*, *5*, 307–328.

Bradford, S. (2005), Godunov-based model for nonhydrostatic wave dynamics, *J. Waterw. Port Coastal Ocean Eng.*, *131*(5), 226–238.

Brocchini, M. (1997), Eulerian and Lagrangian aspects of the longshore drift in the surf and swash zones, *J. Geophys. Res.*, *102*, 23,155–23,169.

Brocchini, M. (2006), Integral swash zone models, *Cont. Shelf Res.*, *26*, 653–660.

Brocchini, M., and G. Bellotti (2002), Integral flow properties of the swash zone and averaging. part 2. The shoreline boundary conditions for wave-averaged models, *J. Fluid Mech.*, *458*, 269–281.

Brocchini, M., and D. Peregrine (1996), Integral flow properties of the swash zone and averaging, *J. Fluid Mech.*, *317*, 241–273.

Butt, T., and P. Russell (1999), Suspended sediment transport mechanism in high-energy swash, *Mar. Geol.*, *161*, 361–375.

Butt, T., and P. Russell (2000), Hydrodynamics and cross-shore sediment transport in the swash-zone of natural beaches: A review, *J. Coastal Res.*, *16*, 255–268.

Calantoni, J., and J. Puleo (2006), Role of pressure gradients in sheet flow of coarse sediments under sawtooth waves, *J. Geophys. Res.*, *111*, C01010, doi:10.1029/2005JC002875.

Casale, C., M. Brocchini, and R. Archetti (2002), Una stima del trasporto solido in prossimità della battigia, in *Atti del XXIX Convegno di Idraulica e Costruzioni Idrauliche*, vol. 3, pp. 721–728, Dip. Ing. Civ. e Ambientale dell'Univ., Univ. degli Stud. di Trento, Trento, Italy.

Coco, G., T. Burnet, B. Werner, and S. Elgar (2003), Test of self-organization in beach cusp formation, *J. Geophys. Res.*, *108*(C3), 3101, doi:10.1029/2002JC001496.

Conley, D., and J. Griffin (2004), Direct measurements of bed shear stress under swash in the field, *J. Geophys. Res.*, *109*, C03050, doi:10.1029/2003JC001899.

Cowen, E., I. Sou, P.-F. Liu, and B. Raubenheimer (2003), Particle image velocimetry measurements within a laboratory-generated swash zone, *J. Eng. Mech.*, *129*, 1119–1129.

Cox, D., W. Hobensack, and A. Sukumaran (2000), Bottom stress in the inner surf and swash zone, in *Coastal Engineering 2000*, vol. 1, edited by B. L. Edge, pp. 108–119, Am. Soc. of Civ. Eng., Reston, Va.

Drake, T., and J. Calantoni (2001), Discrete particle model for sheet flow sediment transport in the nearshore, *J. Geophys. Res.*, *106*, 19,859–19,868.

Duncan, J. (1964), The effects of water table and tide cycle on swash-backwash, sediment distribution and beach profile development, *Mar. Geol.*, *2*, 186–197.

Elfrink, B., and T. Baldock (2002), Hydrodynamics and sediment transport in the swash zone: A review and perspectives, *Coastal Eng.*, *45*, 149–167.

Fraccarollo, L., and H. Capart (2002), Riemann wave description of erosional dam-break flows, *J. Fluid Mech.*, *461*, 183–228.

Fredsoe, J., B. Sumer, A. Kozakiewicz, L. Chua, and R. Deigaard (2003), Effect of externally generated turbulence on wave boundary layer, *Coastal Eng.*, *49*, 155–183.

Grant, U. (1948), Influence of watertable on beach aggradation and degradation, *J. Mar. Res.*, *7*, 655–660.

Grass, A. J., R. R. Simons, R. D. Maciver, M. Mansour-Tehrani, and A. Kalopedis (1995), Shear cell for direct measurements of fluctuating bed shear stress vector in combined wave/current flow, in *Proceedings of XXVIth IAHR Congress: Hydraulic Research and Its Applications Next Century-HYDRA 2000*, vol. 1, pp. 415–420, Int. Assoc. of Hydraul. Eng. and Res., Madrid.

Guard, P., and T. Baldock (2007), The influence of seaward boundary conditions on swash zone hydrodynamics, *Coastal Eng.*, *54*, 321–331.

Guard, P. A., T. Baldock, and P. Nielsen (2005), General solutions for the initial run-up of a breaking tsunami front, in *International Symposium on Disaster Reduction on Coasts* [CD-ROM], Monash Univ., Melbourne, Vic., Australia.

Guza, R., and E. Thornton (1985), Observations of surf beat, *J. Geophys. Res.*, *90*, 3161–3172.

Hasselmann, K. (1971), On the mass and momentum transfer between short gravity waves and larger-scale motions, *J. Fluid Mech.*, *50*, 189–205.

Hibberd, S., and D. Peregrine (1979), Surf and run-up on beaches: A uniform bore, *J. Fluid Mech.*, *95*, 323–345.

Holland, K., and R. Holman (1993), The statistical distribution of swash maxima on natural beaches, *J. Geophys. Res.*, *98*, 10,271–10,278.

Holland, K., and R. Holman (1999), Wavenumber-frequency structure of infragravity swash motions, *J. Geophys. Res.*, *104*, 13,479–13,488.

Holman, R. (1986), Extreme value statistics for wave run-up on a natural beach, *Coastal Eng.*, *9*, 527–544.

Horn, D. (2006), Measurements and modelling of beach groundwater flow in the swash-zone: A review, *Cont. Shelf Res.*, *26*, 622–652.

Hsu, T.-J., and B. Raubenheimer (2006), A numerical and field study on inner-surf and swash sediment transport, *Cont. Shelf Res.*, *26*(5), 589–598.

Hughes, M. (1992), Application of a non-linear shallow water theory to swash following bore collapse on a sandy beach, *J. Coastal Res.*, *8*, 562–578.

Hughes, M. (1995), Friction factors for wave up-rush, *J. Coastal Res.*, *11*, 1089–1098.

Hughes, M., and T. Baldock (2004), Eulerian flow velocities in the swash zone: Field data and model predictions, *J. Geophys. Res.*, *109*, C08009, doi:10.1029/2003JC002213.

Hughes, M., and P. Cowell (1987), Adjustment of reflective beaches to waves, *J. Coastal Res.*, *3*, 153–167.

Hunt, I. (1959), Design of seawalls and breakwaters, *J. Waterw. Harbors Coastal Eng. Div. Am. Soc. Civ. Eng.*, *85*(WW3), 123–152.

Huntley, D., R. Guza, and A. Bowen (1977), A universal form for shoreline run-up spectra, *J. Geophys. Res.*, *82*, 2577–2581.

Jensen, A., G. Pedersen, and D. Wood (2003), An experimental study of wave run-up at a steep beach, *J. Fluid Mech.*, *486*, 161–188.

Johnson, H., T. Karambas, I. Avgeris, B. Zanuttigh, D. Gonzalez-Marco, and I. Caceres (2005), Modelling of waves and currents around submerged breakwaters, *Coastal Eng.*, *52*, 949–969.

King, D. (1991), Studies in oscillatory flow bedload sediment transport, Ph.D. thesis, Univ. of Calif., San Diego, San Diego.

Kobayashi, N., and B. Johnson (2001), Sand suspension, storage, advection, and settling in surf and swash zones, *J. Geophys. Res.*, *106*, 9363–9376.

Kobayashi, N., M. Herrman, B. Johnson, and M. Orzech (1998), Probability distribution of surface elevation in surf and swash zones, *J. Waterw. Port Coastal Ocean Eng.*, *124*(3), 99–107.

Li, Y., and F. Raichlen (2002), Non-breaking and breaking solitary wave run-up, *J. Fluid Mech.*, *456*, 295–318.

Longo, S., M. Petti, and I. Losada (2002), Turbulence in the swash and surf zones: A review, *Coastal Eng.*, *45*, 129–147.

Longuet-Higgins, M., and R. Stewart (1964), Radiation stresses in water waves: A physical discussion, with applications, *Deep Sea Res. Oceanogr. Abstr.*, *11*, 529–562.

Mase, H. (1988), Spectral characteristics of random wave run-up, *Coastal Eng.*, *12*, 175–189.

Mase, H. (1995), Frequency down-shift on swash oscillations compared to incident waves, *J. Hydraul. Res.*, *33*, 397–411.

Masselink, G., and M. Hughes (1998), Field investigation of sediment transport in the swash zone, *Cont. Shelf Res.*, *18*, 1179–1199.

Masselink, G., and J. Puleo (2006), Swash-zone morphodynamics, *Cont. Shelf Res*, *26*, 661–680.
Masselink, G., D. Evans, M. Hughes, and P. Russell (2005), Suspended sediment transport in the swash zone of a dissipative beach, *Mar. Geol.*, *216*, 169–189.
Matsunaga, N., and H. Honji (1980), The backwash vortex, *J. Fluid Mech.*, *99*, 813–815.
Matsunaga, N., and H. Honji (1983), The steady and unsteady backwash vortices, *J. Fluid Mech.*, *135*, 189–197.
Myrhaug, D., L. Holmedal, R. Simons, and R. MacIver (2001), Bottom friction in random waves plus current flow, *Coastal Eng.*, *43*, 75–92.
Nielsen, P. (2002), Shear stress and sediment transport calculations for swash zone modelling, *Coastal Eng.*, *45*, 53–60.
Nielsen, P., and D. Hanslow (1991), Wave runup distributions on natural beaches, *J. Coastal Res.*, *7*, 1139–1152.
Packwood, A. R., and D. H. Peregrine (1981), Surf and runup on beaches: Models of viscous effects, *Rep. AM-81-07*, Sch. of Math., Univ. of Bristol, Bristol, U. K.
Peregrine, D. (1972), Equations for water waves and the approximations behind them, in *Waves on Beaches and the Resulting Sediment Transport*, edited by R. Meyer, pp. 95–121, Academic, New York.
Peregrine, D. (1974), Surface shear waves, *J. Hydraul. Div. Am. Soc. Civ. Eng.*, *100*(HY9), 1215–1227.
Peregrine, D., and S. Williams (2001), Swash overtopping a truncated plane beach, *J. Fluid Mech.*, *440*, 391–399.
Petti, M., and S. Longo (2001), Turbulence experiments in the swash zone, *Coastal Eng.*, *43*, 1–24.
Pritchard, D., and A. Hogg (2005), On the transport of suspended sediment by a swash event on a plane beach, *Coastal Eng.*, *52*, 1–23.
Puleo, J., and K. Holland (2001), Estimating swash zone friction coefficients on a sandy beach, *Coastal Eng.*, *43*, 25–40.
Puleo, J., R. Beach, R. Holman, and J. Allen (2000), Swash zone sediment suspension and transport and the importance of bore-generated turbulence, *J. Geophys. Res.*, *105*, 17,021–17,044.
Raubenheimer, B., S. Elgar, and R. Guza (2004), Observations of swash zone velocities: A note on friction coefficients, *J. Geophys. Res.*, *109*, C01027, doi:10.1029/2003JC001877.
Riedel, P., and J. Kamphuis (1973), A shear plate for use in oscillatory flow, *J. Hydraul. Res.*, *11*, 137–155.
Ruggiero, P., R. Holman, and R. Beach (2004), Wave run-up on a high-energy dissipative beach, *J. Geophys. Res.*, *109*, C06025, doi:10.1029/2003JC002160.
Shen, M., and R. Meyer (1963), Climb of a bore on a beach part 3. Run-up, *J. Fluid Mech.*, *16*, 113–125.
Stockdon, H., R. Holman, P. Howd, and A. J. Sallenger (2006), Empirical parameterization of setup, swash, and runup, *Coastal Eng.*, *53*, 573–588.
Toro, E. (2001), *Shock-Capturing Methods for Free-Surface Shallow Flows*, John Wiley, New York.
Turner, I., and G. Masselink (1998), Swash infiltration-exfiltration and sediment transport, *J. Geophys. Res.*, *103*, 30,813–30,824.
Watson, G., T. Barnes, and D. Peregrine (1994), The generation of low frequency waves by a single wave group incident on a beach, in *Proceedings of 24th International Conference on Coastal Engineering*, vol. 1, pp. 776–790, Am. Soc. of Civ. Eng., New York.
Wei, G., J. Kirby, and A. Sinha (1999), Generation of waves in Boussinesq models using a source function method, *Coastal Eng.*, *36*, 271–299.
Weir, F., M. Hughes, and T. Baldock (2006), Beach face and berm morphodynamics fronting a coastal lagoon, *Geomorphology*, *82*, 331–346.
Whitham, G. (1958), On the propagation of shock waves through regions of non-uniform area or flow, *J. Fluid Mech.*, *4*, 337–360.
Yeh, H. (1991), Tsunami bore runup, *Nat. Hazards*, *4*, 209–220.
Yeh, H. (2006), Maximum fluid forces in the tsunami runup zone, *J. Waterw. Port Coastal Ocean Eng.*, *132*(6), 496–500.
Yeh, H., A. Ghazali, and I. Marton (1989), Experimental study of bore run-up, *J. Fluid Mech.*, *206*, 563–578.

T. E. Baldock, Division of Civil Engineering, University of Queensland, Brisbane, QLD 4072, Australia.
M. Brocchini, Istituto di Idraulica e Infrastrutture Viarie, Università Politecnica delle Marche, Via Brecce Bianche 12, I-60131 Ancona, Italy. (m.brocchini@univpm.it)